

## **Distribution Agreement**

In presenting this thesis or dissertation as a partial fulfillment of the requirements for an advanced degree from Emory University, I hereby grant to Emory University and its agents the non-exclusive license to archive, make accessible, and display my thesis or dissertation in whole or in part in all forms of media, now or hereafter known, including display on the world wide web. I understand that I may select some access restrictions as part of the online submission of this thesis or dissertation. I retain all ownership rights to the copyright of the thesis or dissertation. I also retain the right to use in future works (such as articles or books) all or part of this thesis or dissertation.

Signature:

\_\_\_\_\_  
Marcella Abby Putri

\_\_\_\_\_  
Date

Development of a Redox-Active Ligand Framework: A Novel Approach towards  
Reactivity in C–H Functionalization Reactions

By

Marcella A. Putri

Master of Science

Chemistry

---

Simon B. Blakey  
Advisor

---

Huw M. L. Davies  
Committee Member

---

Nathan T. Jui  
Committee Member

Accepted:

---

Lisa A. Tedesco, Ph.D.  
Dean of the James T. Laney School of Graduate Studies

---

Date

Development of a Redox-Active Ligand Framework: A Novel Approach towards  
Reactivity in C–H Functionalization Reactions

By

Marcella A. Putri  
B.S., Berry College, 2014

Advisor: Simon B. Blakey, Ph.D.

An abstract of  
A thesis submitted to the Faculty of the  
James T. Laney School of Graduate Studies of Emory University  
in partial fulfillment of the requirements for the degree of  
Master of Science  
in Chemistry  
2016

## Abstract

### Development of a Redox-Active Ligand Framework: A Novel Approach towards Reactivity in C–H Functionalization Reactions

By

Marcella A. Putri

The development of C–H functionalization chemistry has advanced significantly in recent years, allowing for more efficient methods for synthesizing complex molecules by forming C–C and C–N bonds from classically unreactive C–H bonds. Although second- and third-row Group IX transition metal catalysts dominate significant portions of the field for C–H functionalization chemistry, recent work by several groups have indicated new reactivity patterns using first-row transition metal catalysts with redox-active ligands. However, limitations to these catalysts include ease of use and inaccessibility. We hypothesize that the use of redox-active ligands with second- and third-row transition metals will allow us to access new reactivity that was previously only accessible by first-row transition metal catalysts. A method for synthesizing a new redox-active ligand scaffold has been developed in our lab. Plans to generate metal complex and assess its viability in C–H functionalization reactions are currently underway.

Development of a Redox-Active Ligand Framework: A Novel Approach towards  
Reactivity in C–H Functionalization Reactions

By

Marcella A. Putri  
B.S., Berry College, 2014

Advisor: Simon B. Blakey, Ph.D.

A thesis submitted to the Faculty of the  
James T. Laney School of Graduate Studies of Emory University  
in partial fulfillment of the requirements for the degree of  
Master of Science  
in Chemistry  
2016

## Table of Contents

|  |           |
|--|-----------|
| <b>Introduction.....</b>   | <b>1</b>  |
| I. Classic Methods to Form C–C and C–N Bonds.....                            | 1         |
| II. Metallocarbenes.....   | 2         |
| III. Metallonitrenes.....  | 7         |
| IV. Emerging Methods in C–C and C–N Bond Formation.....                      | 10        |
| <b>Results and Discussion.....</b>   | <b>16</b> |
| I. C–H Amination with Aryl Azides.....                                       | 16        |
| II. Development of a Redox-Active Ligand Framework.....                      | 20        |
| III. Future Directions.....  | 26        |
| <b>Experimental.....</b>   | <b>28</b> |
| General Information.....   | 28        |
| I. Preparation of Azide <b>7</b> .....                                       | 29        |
| II. Preparation of 5- <i>tert</i> -butyl Phebox Ligands.....                 | 31        |
| III. Preparation of 4- <i>tert</i> -butyl Iridium(III) Phebox Complexes..... | 34        |
| IV. Amination Reaction for Tetrahydroquinoline Formation.....                | 36        |
| V. Preparation of Ligand <b>23</b> .....                                     | 37        |
| VI. HPLC Data.....   | 45        |
| <b>References.....</b>   | <b>46</b> |

## List of Schemes

|   |    |
|---|----|
| <b>Scheme 1.</b> Various methods of C–C bond formation in biologically active molecules....   | 1  |
| <b>Scheme 2.</b> Various methods of C–N bond formation for biologically active molecules...   | 2  |
| <b>Scheme 3.</b> Asymmetric intramolecular and intermolecular C–H insertion with donor/acceptor diazos using Rh(II) tetracarboxylate complexes.....   | 4  |
| <b>Scheme 4.</b> Synthesis of a podophyllotoxin derivative via a 4-substituted $\gamma$ -butyrolactone.....   | 5  |
| <b>Scheme 5.</b> Double C–H insertion reaction to form chiral spiran compounds.....   | 6  |
| <b>Scheme 6.</b> Rh(OAc) <sub>4</sub> catalyzed C–H insertion versus cyclopropanation using acceptor-only and acceptor/acceptor diazo compounds.....  | 7  |
| <b>Scheme 7.</b> C–H amination of sulfamates and sulfamides to form amine compounds.....  | 8  |
| <b>Scheme 8.</b> Du Bois' synthesis of (–)-tetrodotoxin via a key C–H amination step.....   | 8  |
| <b>Scheme 9.</b> C–H amination of sulfonyl azides using Rh(II)- and Ir(III)-catalysts.....  | 9  |
| <b>Scheme 10.</b> Driver's Ir-catalyzed C–H amination of aryl azides and enantioselective Ir-catalyzed C–H amination (Nina Weldy and Clay Owens)..... | 10 |
| <b>Scheme 11.</b> C–H amination of aryl azides using Co(II) complex with redox-active ligand framework.....   | 11 |
| <b>Scheme 12.</b> Acceptor/acceptor and acceptor-only diazo reactions catalyzed by Zhang's Co(II)-por* catalyst.....                                  | 12 |
| <b>Scheme 13.</b> C–H amination of alkyl azides using Fe(II) complex with a redox-active ligand.....  | 13 |

|  |    |
|--|----|
| <b>Scheme 14.</b> 1,2-hydride shifts with A) alkyl azides and B) $\alpha$ -alkyl- $\alpha$ -diazoacetates.....               | 14 |
| <b>Scheme 15.</b> Enantioselective C–H insertion with $\alpha$ -alkyl- $\alpha$ -diazoacetates.....                          | 15 |
| <b>Scheme 16.</b> C–H amination of aryl azide <b>7</b> using Ir(III)-phebox catalyst.....                                    | 16 |
| <b>Scheme 17.</b> Synthesis of azide <b>7</b> .....  | 17 |
| <b>Scheme 18.</b> Synthesis of Ir- <sup><i>i</i></sup> Pr-phebox catalysts.....  | 18 |
| <b>Scheme 19.</b> C–H amination using racemic catalyst and enantiopure catalyst.....   | 18 |
| <b>Scheme 20.</b> Attempted synthesis of catalyst <b>16</b> .....  | 19 |
| <b>Scheme 21.</b> C–H amination to form indoline <b>17</b> (Nina Weldy) and tetrahydroquinoline <b>8</b><br>(this work)..... | 20 |
| <b>Scheme 22.</b> Synthesis of ligand <b>23</b> .....  | 21 |
| <b>Scheme 23.</b> Ortho Buchwald-Hartwig diamination using aniline-derived substrate and<br>alkyl amine substrate.....       | 22 |
| <b>Scheme 24.</b> Attempted metallation of <b>23</b> .....   | 26 |

## List of Figures

|  |    |
|--|----|
| <b>Figure 1.</b> Classifications of diazo compounds.....   | 3  |
| <b>Figure 2.</b> Proposed metalloradical mechanism for cyclopropanation of diazo compounds.....                    | 13 |
| <b>Figure 3.</b> $^1\text{H}$ NMR spectra of Buchwald-Hartwig coupling products compared to starting material..... | 24 |
| <b>Figure 4.</b> Proposed Group IX complexes.....  | 25 |
| <b>Figure 5.</b> Mosher amide analysis for absolute configuration of amine <b>22</b> .....                         | 41 |

## List of Tables

|  |    |
|--|----|
| <b>Table 1.</b> Initial optimization efforts of the Buchwald-Hartwig coupling..... | 23 |
|--|----|

## Abbreviations

|        |  |
|--------|--|
| Ac     | acetyl                                   |
| AcOH   | acetic acid                              |
| Boc    | <i>tert</i> -butoxycarbonyl              |
| Bn     | benzyl                                   |
| br     | broad                                    |
| d      | doublet                                  |
| dba    | dibenzylideneacetone                     |
| DCM    | dichloromethane                          |
| DMF    | <i>N, N'</i> -dimethylformamide          |
| DMSO   | dimethylsulfoxide                        |
| equiv. | equivalent                               |
| ESI    | electrospray ionization                  |
| EtOAc  | ethyl acetate                            |
| HRMS   | high resolution mass spectroscopy        |
| LiHMDS | lithium <i>bis</i> (trimethylsilyl)amide |
| m      | multiplet                                |
| mmol   | millimole                                |
| Ms     | methanesulfonyl                          |
| NMR    | nuclear magnetic resonance               |
| Ph     | phenyl                                   |
| phebox | bis(oxazoliny)phenyl                     |

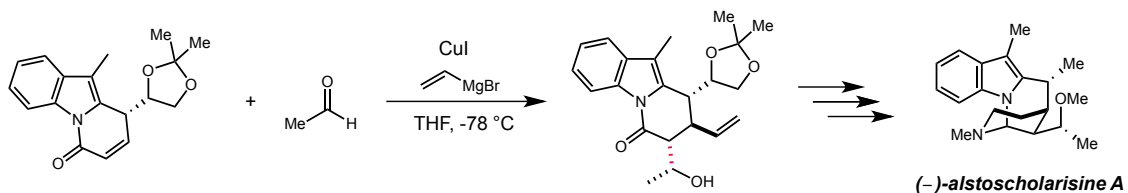
|       |                                 |
|-------|---------------------------------|
| ppm   | parts per million               |
| q     | quartet                         |
| quint | quintet                         |
| rt    | room temperature                |
| s     | singlet                         |
| t     | triplet                         |
| TBME  | <i>tert</i> -butyl methyl ether |
| TBDMS | <i>tert</i> -butyldimethylsilyl |
| TBDPS | <i>tert</i> -butyldihenylsilyl  |
| Tf    | trifluoromethanesulfonyl        |
| TFA   | trifluoroacetic acid            |
| THF   | tetrahydrofuran                 |
| TMS   | trimethylsilyl                  |
| Ts    | <i>para</i> -toluenesulfonyl    |

## Introduction

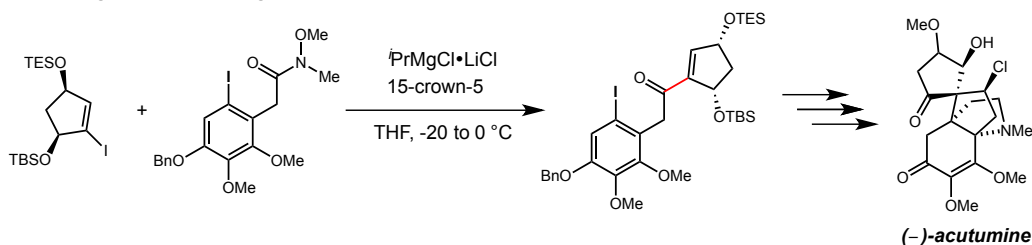
### I. Classic Methods to Form C–C and C–N Bonds

The formation of carbon–carbon and carbon–nitrogen bonds has been a major focus in the field of synthetic organic chemistry, especially towards the goal of forming pharmaceutically relevant molecules. Some of the classic methods developed to form C–C bonds include the aldol reaction, addition of organometallic reagents, and the Diels Alder reaction (Scheme 1).<sup>1-3</sup>

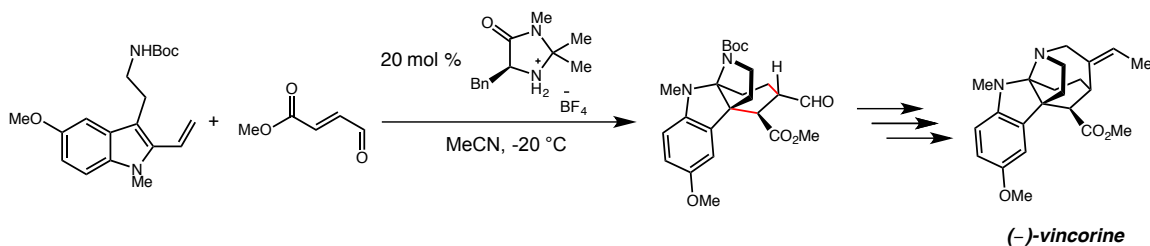
#### A: Aldol Reaction



#### B: Addition of Organometallic Reagent

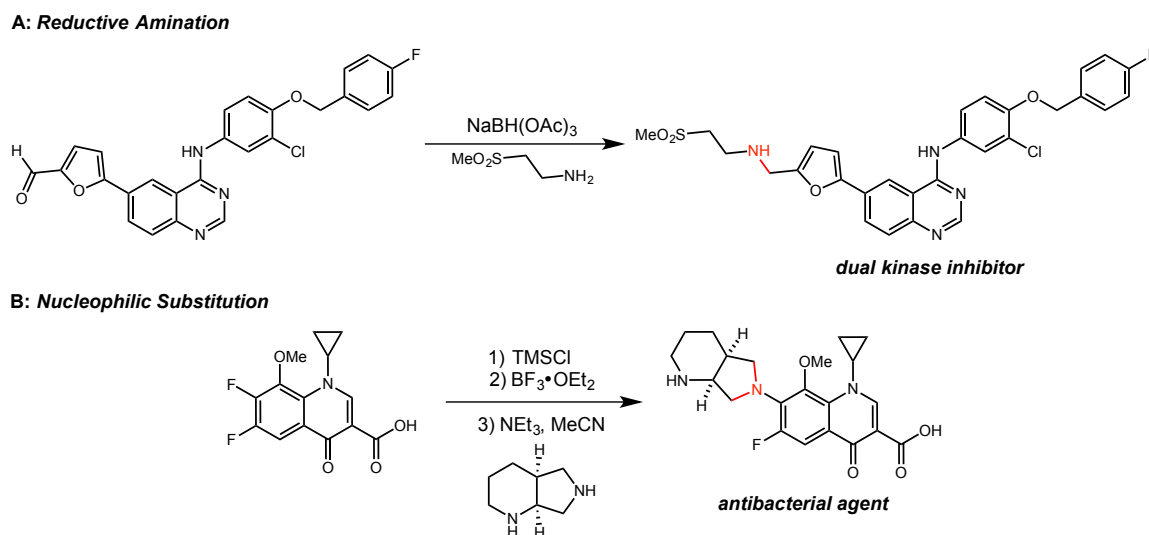


#### C: Diels Alder Reaction



**Scheme 1.** Various methods of C–C bond formation in biologically active molecules.

C–N bond formation is also synthetically important, since many biologically active molecules contain nitrogen. Classic methods developed to form these bonds include reductive amination and nucleophilic substitution (Scheme 2).<sup>4</sup>



**Scheme 2.** Various methods of C–N bond formation for biologically active molecules.

While well developed and robust, these methods require prefunctionalization of the starting materials, resulting in an increased number of reactions needed to form the target molecule and an increase in chemical waste. An attractive solution includes moving towards the direct generation of C–C and C–N bonds directly from classically unreactive C–H bonds via metalcarbene and metallonitrene chemistry, respectively.

## II. Metalcarbenes

One attractive way to access metalcarbenes is via metal-mediated diazo decomposition. The reactivity of metalcarbenes has been observed to correspond to the

electronic nature of the substituents on the metallocarbene: electron-withdrawing groups on the parent diazo-containing compound increase the electrophilicity of the reactive metallocarbene, while electron-donating groups temper that reactivity. The three commonly known types of carbene precursor are acceptor/acceptor, acceptor-only, and donor/acceptor diazo compounds (Figure 1).<sup>5</sup> Acceptor/acceptor diazo compounds consist of two electron-withdrawing groups, rendering the resulting metallocarbene to be extremely electrophilic; acceptor-only diazo compounds have one electron-withdrawing group, while donor/acceptor diazo compounds have an electron-donating group in addition to one electron-withdrawing group to lessen the electrophilicity of the metallocarbene.

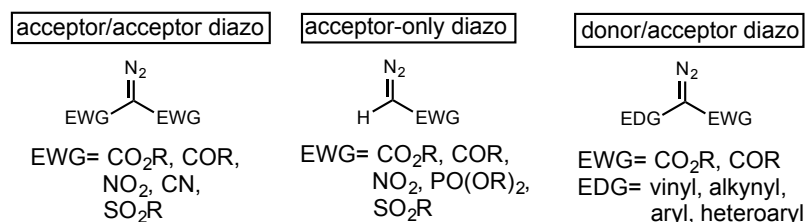
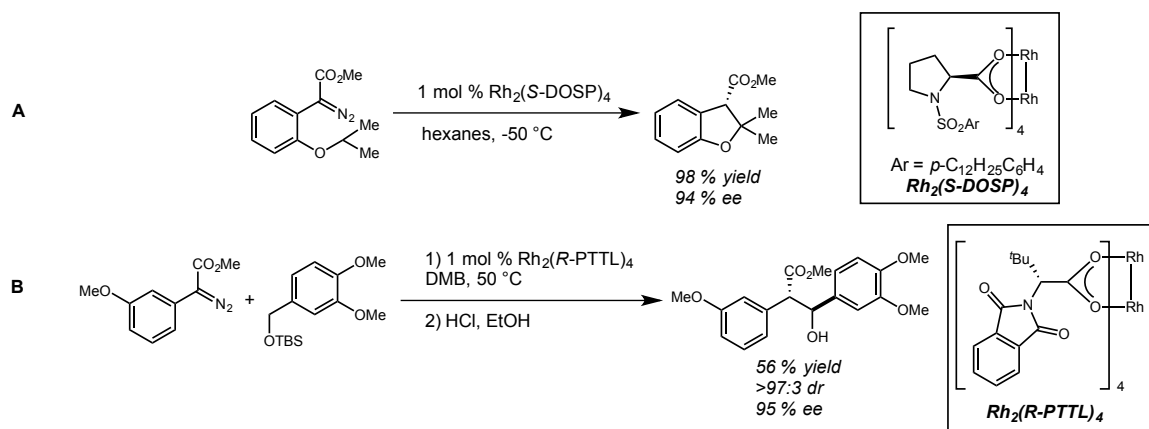


**Figure 1.** Classifications of diazo compounds.

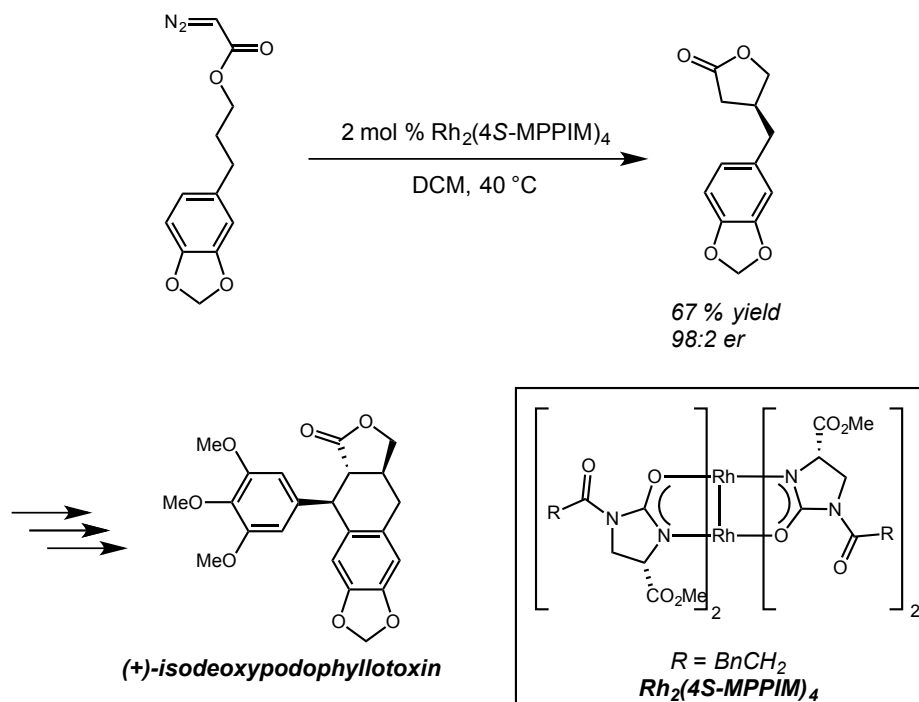
Donor/acceptor diazo compounds are the most widely studied family of diazo-containing species due to the ability of the donor group to moderate the electrophilicity of the metallocarbene, which leads to more selective C–H functionalization reactions. A range of chiral dirhodium(II) tetracarboxylate complexes developed by the Davies<sup>6</sup> and Hashimoto<sup>7</sup> groups have been shown to successfully catalyze a variety of intra- and

intermolecular C–H insertion reactions with donor/acceptor diazo compounds (Scheme 3).



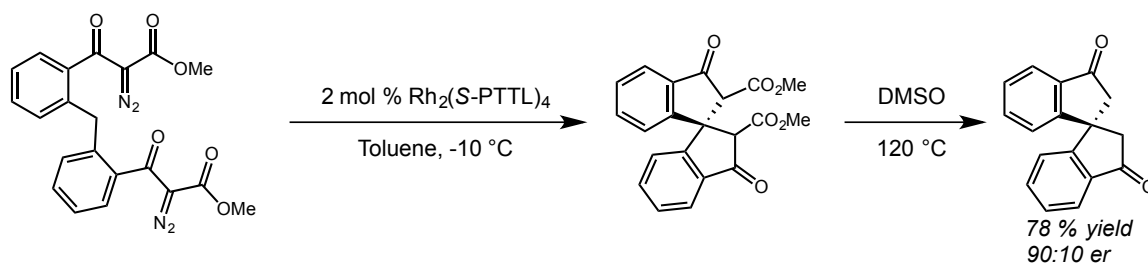
**Scheme 3.** Asymmetric A) intramolecular and B) intermolecular C–H insertion with donor/acceptor diazos using Rh(II) tetracarboxylate complexes.

Acceptor/acceptor and acceptor-only diazo compounds have been studied to a lesser extent due to their highly electrophilic nature, leading to low selectivity within intermolecular C–H functionalization reactions. Moreover, carbene dimerization remains a major competing reaction, necessitating the slow addition of diazo compound. Historically, only intramolecular reactions using acceptor-only diazo compounds afforded high levels of stereocontrol.<sup>8</sup> Doyle's chiral dirhodium(II) carboxamidate complexes have shown to successfully synthesize 4-substituted  $\gamma$ -butyrolactones, which has been utilized in the synthesis of biologically active molecules (Scheme 4).<sup>9</sup>



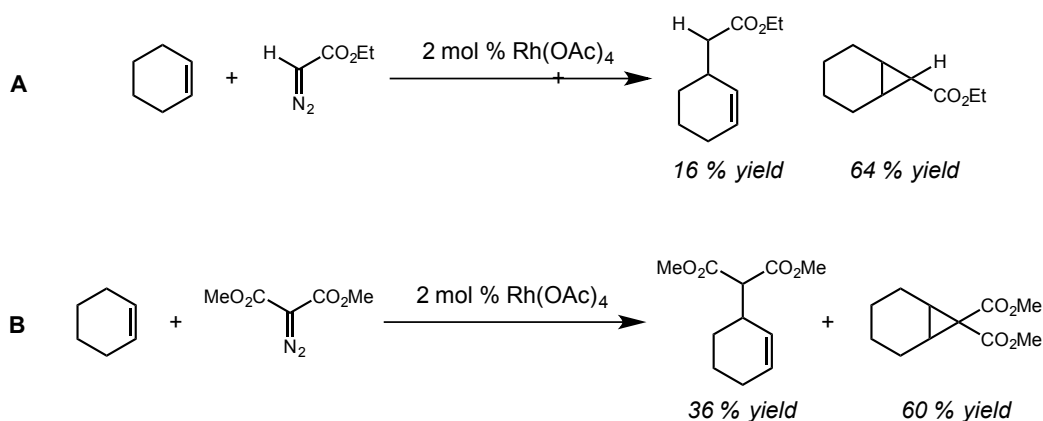
**Scheme 4.** Synthesis of a podophyllotoxin derivative via a 4-substituted  $\gamma$ -butyrolactone.

Studies on intramolecular C–H functionalization reactions of acceptor/acceptor-substituted diazo compounds have been dominated by Ikegami and Hashimoto’s family of *N*-phthaloyl amino acid-based dirhodium(II) carboxylate catalysts.<sup>5</sup> Their dirhodium catalyst  $\text{Rh}_2(S\text{-PTTL})_4$  was able to synthesize chiral spiran compounds via a double C–H insertion reaction using  $\alpha$ -diazo- $\beta$ -ketoesters, giving high yield and moderate enantioselectivity (Scheme 5).<sup>10</sup>



**Scheme 5.** Double C–H insertion reaction to form chiral spiran compounds.

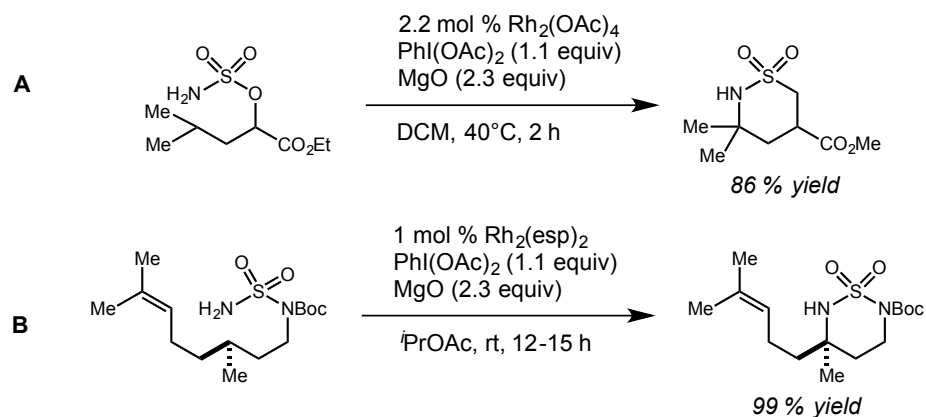
Investigations on an enantioselective intermolecular variant of the C–H insertion reaction using acceptor-only and acceptor/acceptor diazo compounds have been scarce due to their increased electrophilicity compared to their donor/acceptor counterpart. Moreover, studies conducted by the Müller group indicated that chemoselectivity with these diazo-containing compounds can be difficult to control. For example, cyclopropanation is a major competing reaction with C–H functionalization when reacting cyclohexene with acceptor-only or acceptor/acceptor diazo compounds in the presence of Rh(II) catalysts (Scheme 6).<sup>11</sup>



**Scheme 6.** Rh(OAc)<sub>4</sub> catalyzed C–H insertion versus cyclopropanation using A) acceptor-only and B) acceptor/acceptor diazo compounds.

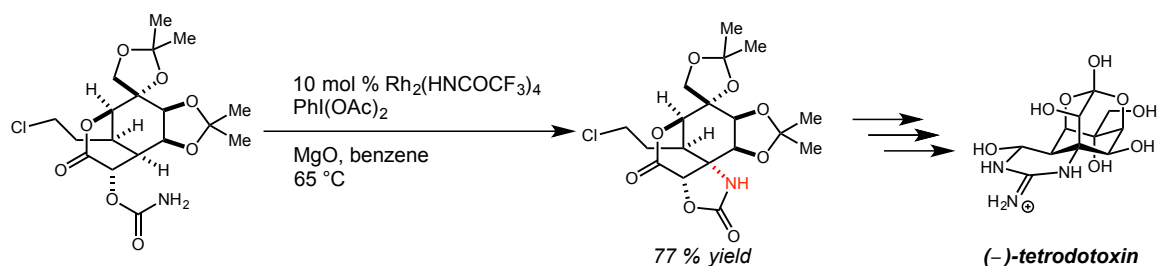
### III. Metallonitrenes

Although studied to a lesser extent compared to their metallocarbene counterpart, progress in the field of C–H amination through metallonitrene chemistry has been made using a variety of nitrene precursors such as carbamates, sulfamates, sulfamides, and sulfonamides (Scheme 7).<sup>12,13</sup> The Du Bois group found that sulfamates could intramolecularly form C–N bonds to generate cyclic oxathiazinanes using a dimeric rhodium catalyst (Scheme 7a); the resulting oxathiazinanes are useful precursors for 1,3-amino alcohols and  $\beta$ -amino acids. In addition to sulfamates, sulfamides were also found to successfully insert into C–H bonds (Scheme 7b).



**Scheme 7.** C–H amination of A) sulfamates and B) sulfamides to form amine compounds.

Du Bois has also highlighted the synthetic utility of C–H amination in pharmaceutically relevant syntheses through his synthesis of (–)-tetradotoxin, forming the C–N bond from a carbamate in a late-stage reaction for a synthetically complex molecule (Scheme 8).<sup>14</sup>

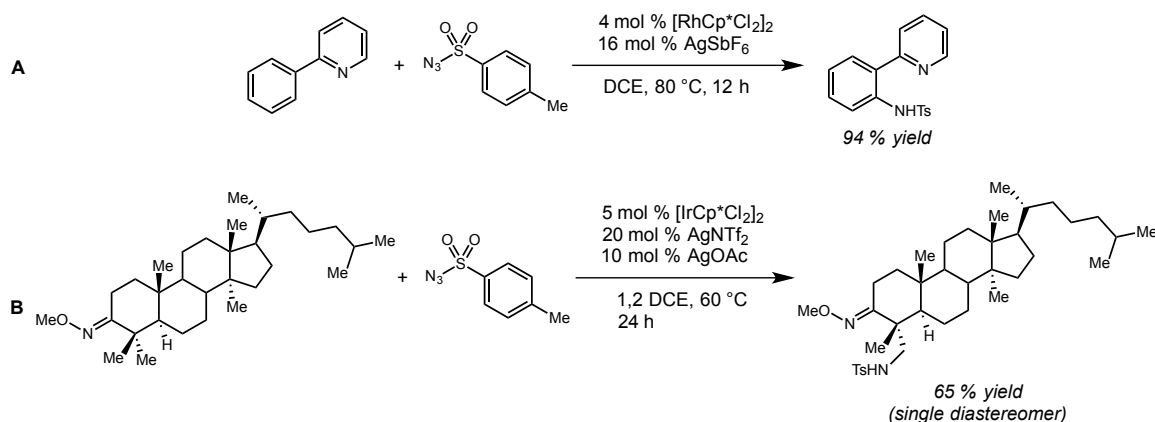


**Scheme 8.** Du Bois' synthesis of (–)-tetradotoxin via a key C–H amination step.

Nevertheless, the products of these reactions often require subsequent modifications to achieve the final desired amine product, and these reactions also require

stoichiometric oxidants. Azides as metallonitrene precursors are an attractive solution to this problem, since using azide-containing substrates would provide the amine product with nitrogen gas as the sole byproduct without the need for external oxidants.

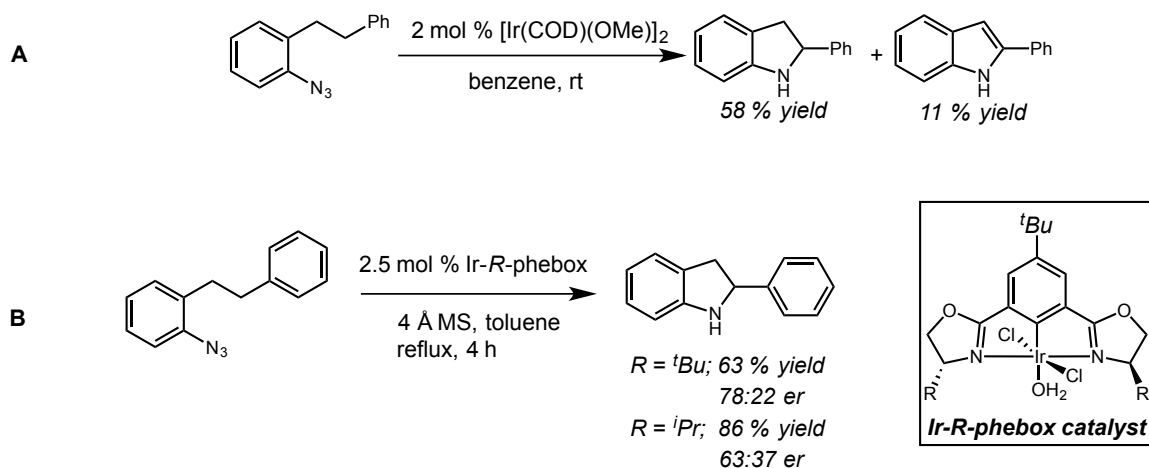
Sulfonyl azides are one particular class of azides that have proved to be useful for C–H aminations. Work by the Chang group in 2012 found that  $[\text{RhCp}^*\text{Cl}_2]_2$  could intermolecularly amidate arenes using sulfonyl azides (Scheme 9a).<sup>15</sup> They expanded this methodology to include an Ir-catalyzed system with mild conditions that allowed for late-stage functionalization of an unactivated methyl group (Scheme 9b).<sup>16</sup> This system also included a broad substrate scope and tolerated a variety of functional groups. However, deprotection of the resulting amine products is still required.



**Scheme 9.** C–H amination of sulfonyl azides using A) Rh(II)- and B) Ir(III)-catalysts.

Investigations into the reactivity of unactivated azides remain limited. In 2009, the Driver group reported a system using  $[\text{Ir}(\text{COD})(\text{OMe})_2]$  to catalyze an intramolecular  $\text{sp}^3$  C–H amination using aryl azides to form indolines (Scheme 10a).<sup>17</sup> Of note, stereocontrol in this intramolecular aryl azide C–H functionalization method is still

largely unaddressed with azides containing no electron-withdrawing groups. However, unpublished results from Nina Weldy and Clay Owens in the Blakey lab indicate that Ir(III)-phebox catalysts are capable of catalyzing moderately enantioselective C–H amination reactions with aryl azides to form the corresponding indoline (Scheme 10b).<sup>18</sup>

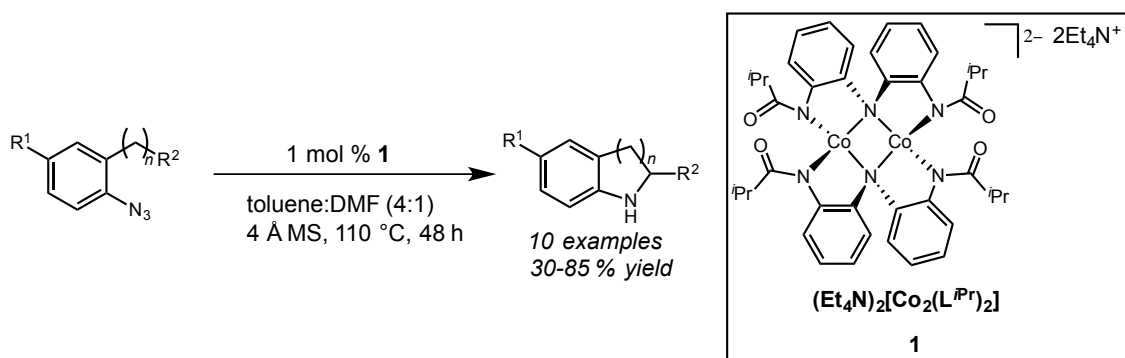


**Scheme 10.** A) Driver's Ir-catalyzed C–H amination of aryl azides and B) enantioselective Ir-catalyzed C–H amination (Nina Weldy and Clay Owens).

#### IV. Emerging Methods in C–C and C–N Bond Formation

Despite the progress that has been made in C–C and C–N bond formation from C–H bonds, second- and third-row Group IX transition metal catalysts dominate significant portions of the field for C–H functionalization chemistry. This is partly due to the metals' ability to further interact with the carbene center through  $\pi$ -backbonding compared to first-row transition metals, allowing for greater selectivity while maintaining electrophilicity.<sup>5</sup>

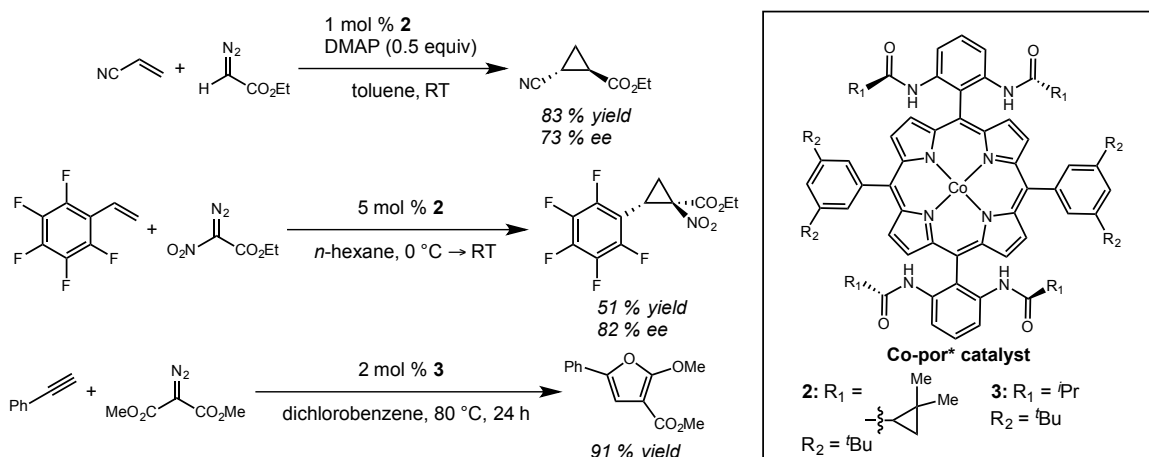
However, recent work by the Blakey group in collaboration with the MacBeth group reported that Co(II) complex **1** with a redox-active ligand scaffold was capable of catalyzing C–H amination reactions of aryl azides that tolerated a variety of functional groups to form 5-, 6-, and 7-membered nitrogen-containing rings in up to 85 % yield (Scheme 11).<sup>19</sup>



**Scheme 11.** C–H amination of aryl azides using Co(II) complex with redox-active ligand framework.

Additionally, the Zhang group has disclosed a chiral Co(II)-porphyrin complex that exhibits novel reactivity in group transfer chemistry involving acceptor-only and acceptor diazo compounds with high levels of stereocontrol (Scheme 12).<sup>20-29</sup> These reactions include cyclopropanation, cyclopropanation, furan formation, and C–H alkylation. This chemistry is chemoselective and highly tolerant of other reactive functional groups. Several remarkable aspects of this Co-porphyrin system include: no slow addition of diazo required, the olefin is the limiting reagent, and little diazo dimerization is observed. Moreover, electron-poor olefins have been shown to

successfully participate in these reactions, despite the highly electrophilic nature of the acceptor/acceptor and acceptor-only Group IX metallocarbene intermediates.



**Scheme 12.** Acceptor/acceptor and acceptor-only diazo reactions catalyzed by Zhang's Co(II)-por\* catalyst.

Rather than the conventional two-electron chemistry that Rh and Ir catalysts are proposed to undergo with donor/acceptor diazo compounds,<sup>30</sup> Zhang proposes that his Co catalyst promotes one-electron metalloradical chemistry, providing an alternative reactivity pathway (Figure 2).<sup>26</sup> After forming the Co(II)-metallocarbene intermediate, Zhang proposes that Co(II) undergoes a one-electron transfer to generate a Co(III)-carbene radical intermediate. In particular, rather than the typical electrophilic metallocarbene intermediate, the proposed radical metallocarbene intermediate behaves more as a nucleophile, capable of attacking electron-poor olefins.

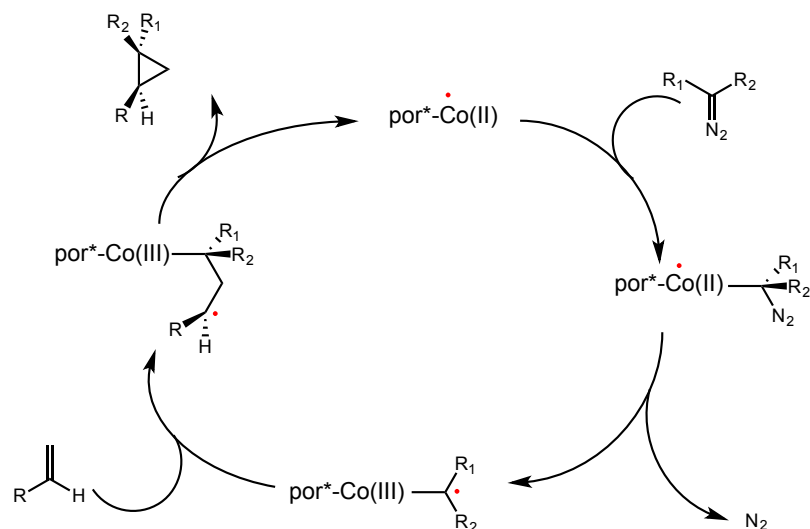
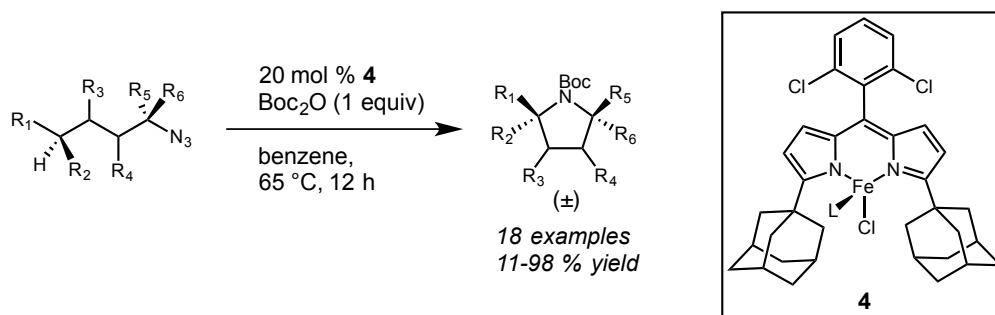


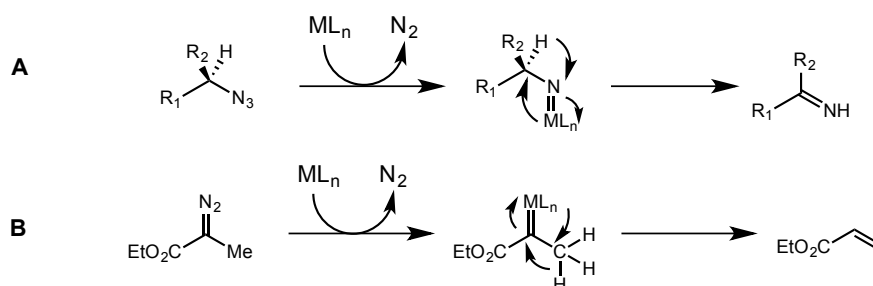
**Figure 2.** Proposed metalloradical mechanism for cyclopropanation of diazo compounds.

In addition to Co(II) complexes, a Fe(II) complex from the Betley group has shown remarkable reactivity with regards to intramolecular C–H amination using alkyl azides (Scheme 13).<sup>31</sup>



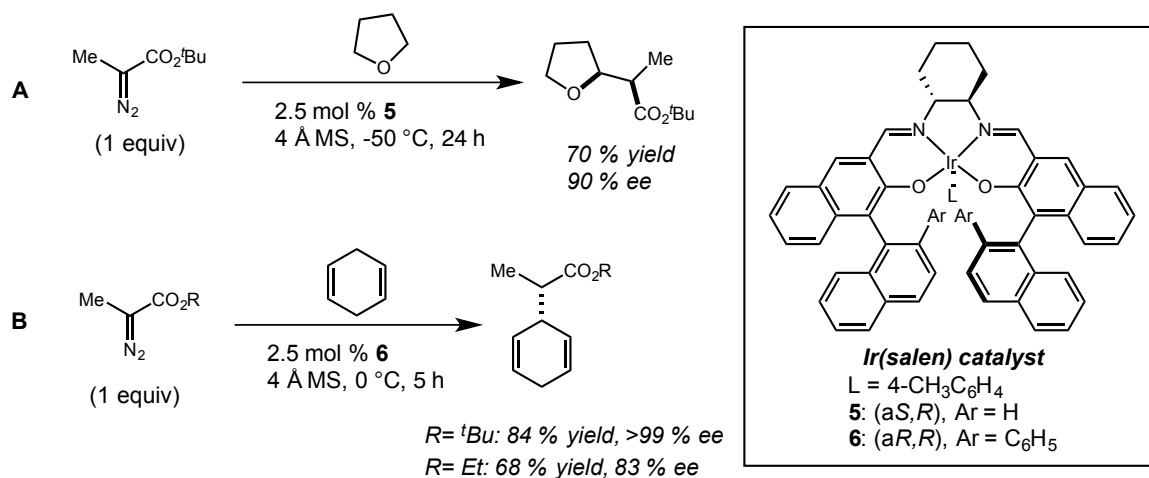
**Scheme 13.** C–H amination of alkyl azides using Fe(II) complex with a redox-active ligand.

This is uncommon because the alkyl-substituted metallonitrene intermediate typically undergoes a 1,2-hydride shift to form the corresponding imine product (Scheme 14a). However, the Betley group was able to avoid this side reaction to successfully form the C–H amination product. Their proposed mechanism also suggests a metalloradical pathway, precluding the two-electron hydride shift in the metallonitrene intermediate.



**Scheme 14.** 1,2-hydride shifts with A) alkyl azides and B)  $\alpha$ -alkyl- $\alpha$ -diazoacetates.

A similar hydride shift also occurs with  $\alpha$ -alkyl- $\alpha$ -diazoacetate compounds, where the resulting metalcarbene intermediate undergoes a facile 1,2-hydride shift to form the corresponding  $\alpha$ ,  $\beta$ -unsaturated ester (Scheme 14b). However, work from the Katsuki group has shown that their Ir(III)-salen complex is capable of doing enantioselective C–H insertion into both THF and 1,4-cyclohexadiene using  $\alpha$ -alkyl- $\alpha$ -diazoacetates (Scheme 15).<sup>32,33</sup>



**Scheme 15.** Enantioselective C–H insertion with  $\alpha$ -alkyl- $\alpha$ -diazoacetates.

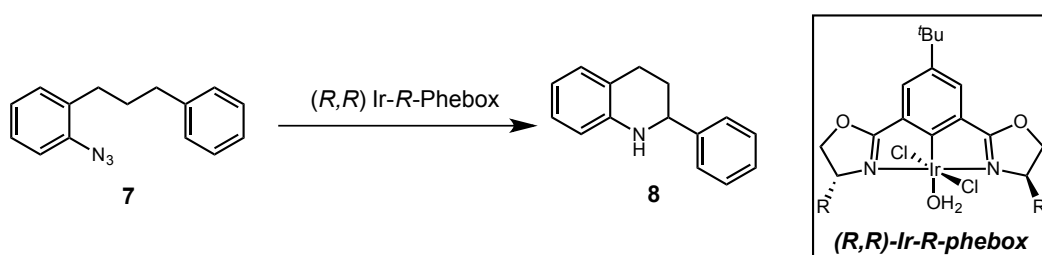
Although the mechanism of this reaction is still unknown, the redox-active salen ligand is speculated to play a major role in this novel reactivity. Katsuki's Ir(III)-salen complex marks the only known third-row transition metal catalyst capable of mimicking the reactivity that the previously mentioned first-row transition metal catalysts displayed. However, a major limitation to this system is the 13-step sequence needed to synthesize the salen ligand.

With this information in hand, we hypothesize that the use of redox-active ligands with second- and third-row transition metals will allow us to access new reactivity that was previously only accessible by first-row transition metal catalysts. Our focus turned towards building a modular and chiral redox-active ligand framework that is easily accessible and convenient to handle with the potential to induce enantioselective radical-type reactivity of carbenes and nitrenes.

## Results and Discussion

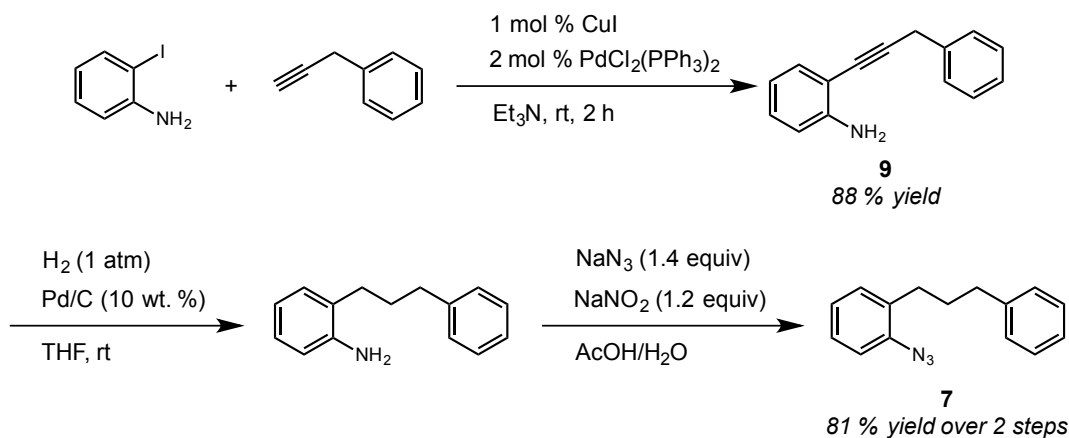
### I. C–H Amination with Aryl Azides

Before moving towards the development of a redox-active ligand framework, our initial studies focused on the stereocontrolling abilities of the Ir(III)-phebox catalyst in forming tetrahydroquinoline **8** from azide **7** (Scheme 16).



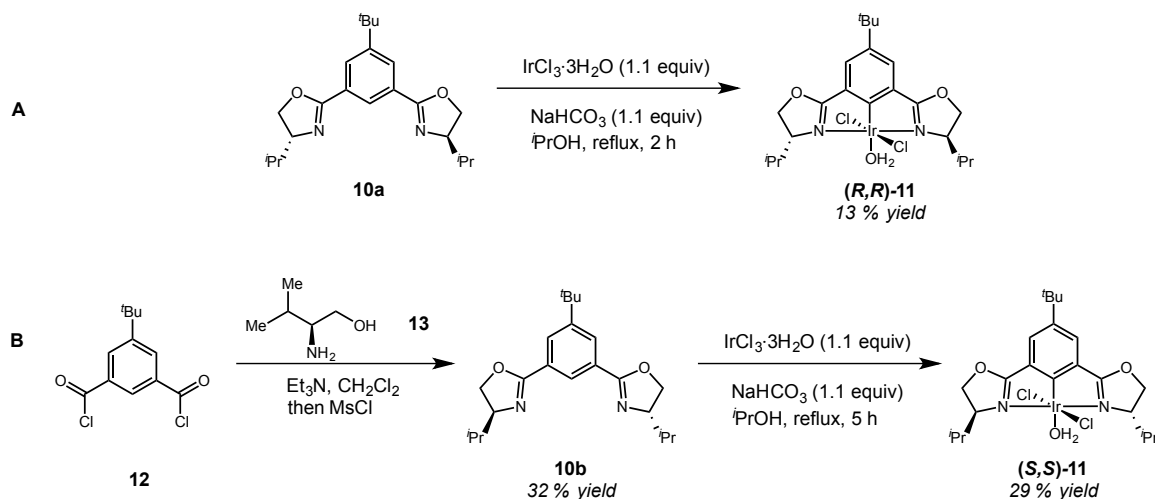
**Scheme 16.** C–H amination of aryl azide **7** using Ir(III)-phebox catalyst.

We hypothesized that the formation of the 6-membered ring would cause a change in transition state geometry, allowing for more useful levels of enantioenrichment. Azide **7** was synthesized using a route described by the Driver group (Scheme 17).<sup>17</sup> A Sonogashira coupling between 2-iodoaniline and 3-phenyl-1-propyne led to **9**,<sup>34</sup> and subsequent hydrogenation followed by azidation afforded the aryl azide in good yield (81 % over two steps).



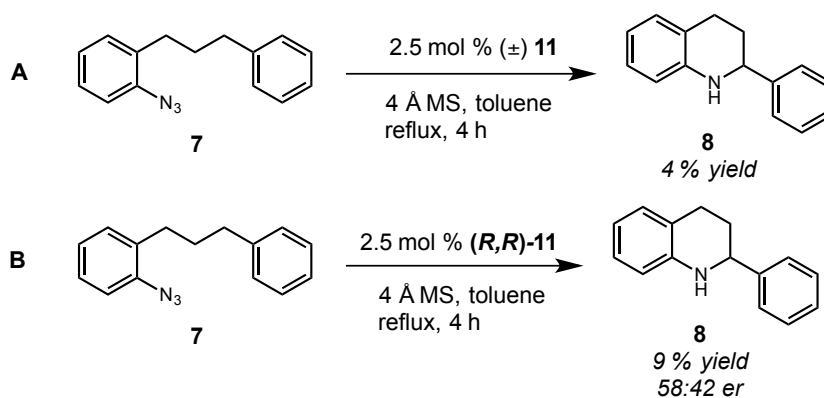
**Scheme 17.** Synthesis of azide **7**.

A racemic mixture of Ir-phebox catalyst **11** was synthesized in order to determine an HPLC assay of the two enantiomeric products.<sup>35</sup> Readily available phebox ligand **10a** was metallated with  $\text{IrCl}_3 \cdot 3\text{H}_2\text{O}$  and  $\text{NaHCO}_3$  under our established reaction conditions (Scheme 18a). Recrystallization by slow diffusion of pentane into a saturated  $\text{CH}_2\text{Cl}_2$  solution gave catalyst (*R,R*)-**11** in 13 % yield. The other enantiomer was synthesized by reacting 5-(*tert*-butyl)isophthaloyl dichloride **12** with (*S*)-amino alcohol **13** to form the corresponding amide; subsequent mesylation with methanesulfonyl chloride and cyclization gave phebox ligand **10b** (32 % yield, Scheme 18b). Subsequent metallation under the standard conditions gave (*S,S*)-**11** in 29 % yield.



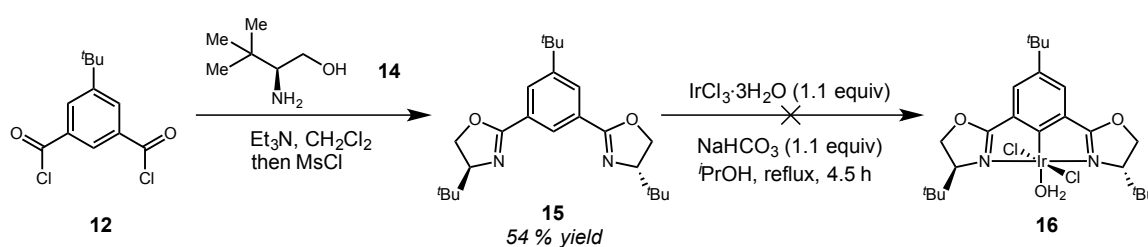
**Scheme 18.** Synthesis of Ir-*i*Pr-phebox catalysts.

Combining equal mixtures of catalysts (*R,R*)-**11** and (*S,S*)-**11** gave the racemic catalyst mixture **11**, which was then utilized in the C–H amination reaction with azide **7** to form tetrahydroquinoline **8** (Scheme 19a). HPLC retention times were observed to be 5.52 min and 13.71 min. C–H amination with azide **7** using catalyst (*R,R*)-**11** gave **8** in 9 % yield (Scheme 19b), and HPLC analysis indicated an enantiomeric ratio of 58:42.



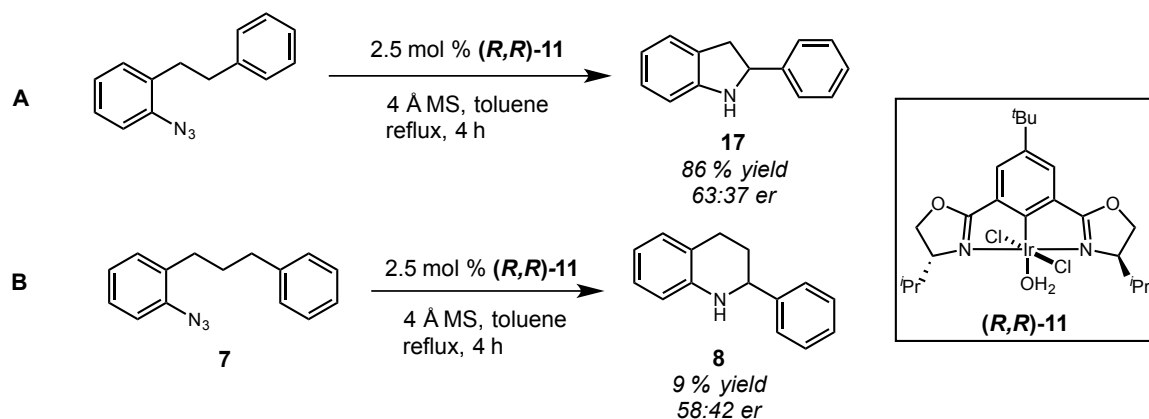
**Scheme 19.** C–H amination using A) racemic catalyst and B) enantiopure catalyst.

An attempt to synthesize Ir-<sup>t</sup>Bu-phebox catalyst **16** was made in order to directly compare the enantioselectivities from the previously synthesized 5-membered cyclized product and the 6-membered cyclized product (Scheme 20). However, efforts to synthesize and purify **16** proved to be challenging. We then moved to instead directly compare the readily available Ir-<sup>i</sup>Pr-phebox catalyst in its abilities to exert enantiocontrol in forming tetrahydroquinoline **8** versus its indoline analog.



**Scheme 20.** Attempted synthesis of catalyst **16**.

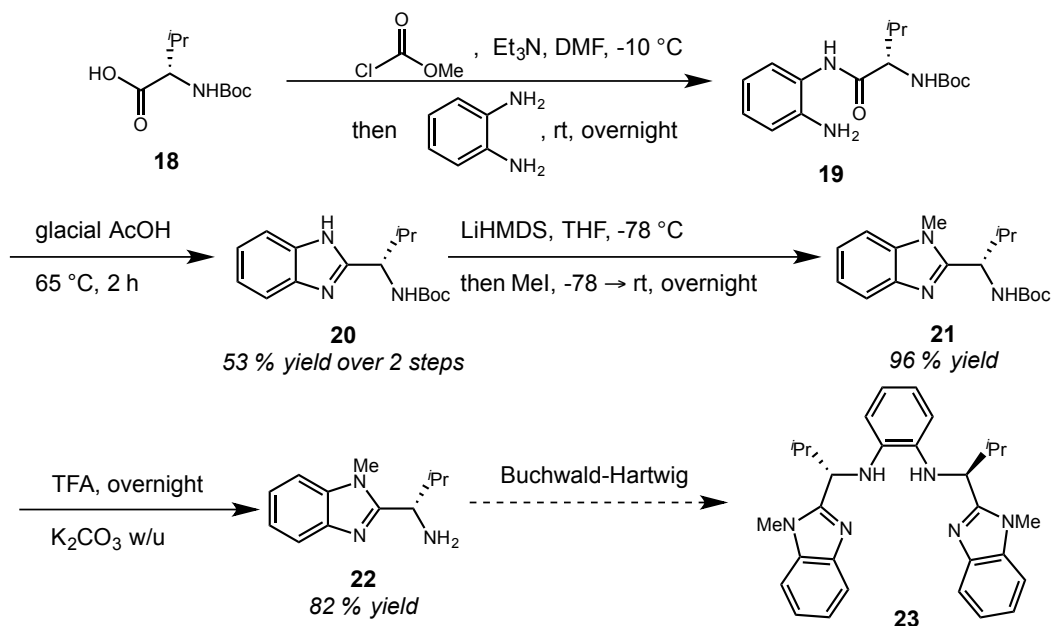
Because the enantioselectivity and yield given by Ir-<sup>i</sup>Pr-Phebox for tetrahydroquinoline **8** were much lower than found for formation of indoline **17** (Scheme 21), we decided to explore alternative ligand scaffolds that have the potential to better control the enantioselectivity of this reaction and other C–H functionalization reactions.



**Scheme 21.** C–H amination to form A) indoline **17** (Nina Weldy) and B) tetrahydroquinoline **8** (this work).

## II. Development of a Redox-Active Ligand Framework

In particular, we were inspired by previous work using Group IX catalysts with redox-active ligands. Therefore, we set out to prepare a readily accessible chiral redox-active tetradentate ligand that could be easily tuned with a variety of substituents. This led to the design of a benzimidazole-based ligand **23** where chirality is easily introduced through a precursor amino acid **18**. Our proposed ligand is synthetically available in five steps, culminating in an ortho Buchwald-Hartwig diamination using a known methylated benzimidazole substrate **22** (Scheme 22).<sup>36</sup>

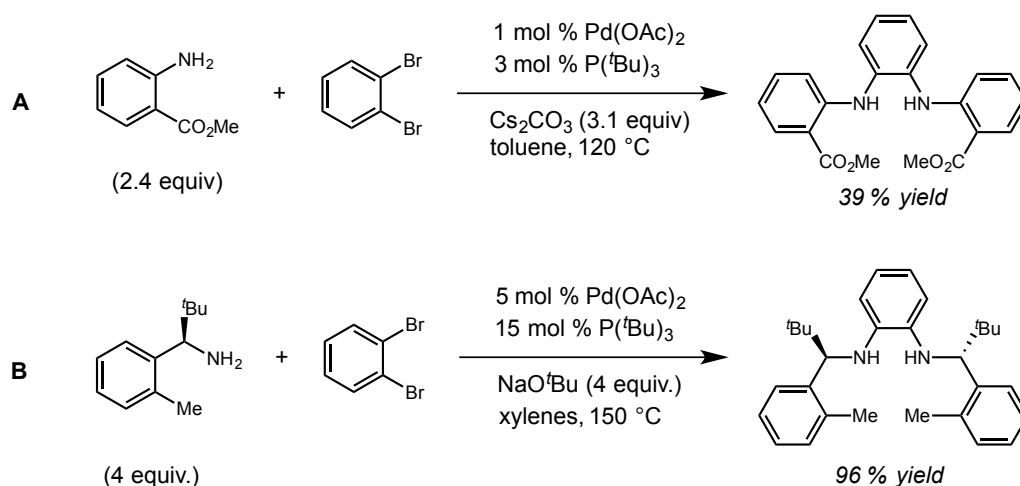


**Scheme 22.** Synthesis of ligand **23**.

The synthesis of ligand **23** began by reacting *o*-phenylenediamine and the commercially available Boc-protected chiral amino acid **18** via a mixed anhydride intermediate, giving amide **19** (Scheme 22). Subsequent cyclization to generate benzimidazole **20** was achieved through a condensation reaction using warm glacial acetic acid, giving **20** in 53 % yield over two steps. *N*-methylation via chemoselective deprotonation using lithium hexamethyldisilazide followed by addition of methyl iodide gave *N*-methylated benzimidazole **21** in 96 % yield. Subsequent Boc deprotection using trifluoroacetic acid and work-up with sodium bicarbonate afforded the Buchwald-Hartwig precursor amine **22** as the proposed free base.

We then turned our attention to the ortho Buchwald-Hartwig diamination reaction to generate our redox-active scaffold system. Previous work done by the Gao group indicated that the ortho Buchwald-Hartwig diamination reaction is possible using an

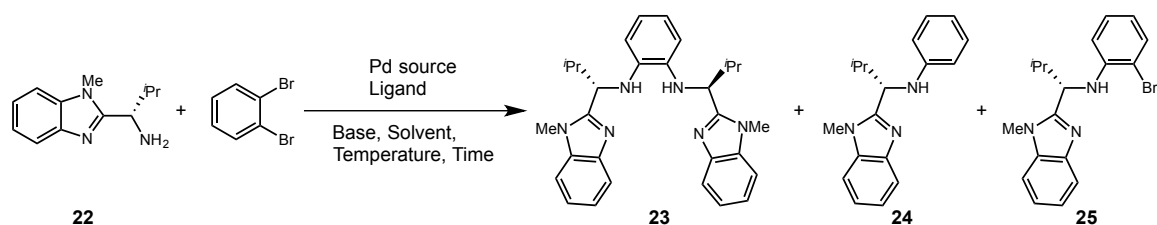
aniline-derived amine, palladium(II) acetate, tri-*tert*-butyl phosphine, and cesium carbonate (Scheme 23a).<sup>37</sup> Moreover, work by the Kündig group yielded a comparable system using a primary amine attached to a hindered benzylic carbon, which is more similar to the nature of our amine substrate. However, their system required the stronger base sodium *tert*-butoxide, higher reaction temperature, and additional equivalents of amine (Scheme 23b).<sup>38</sup>



**Scheme 23.** Ortho Buchwald-Hartwig diamination using A) aniline-derived substrate and B) alkyl amine substrate.

With these literature precedents in mind, we had taken what was the proposed free base and attempted the coupling reactions. However, inconsistencies in later attempts to synthesize **22** led to the discovery that an aqueous sodium bicarbonate wash yielded the ammonium-trifluoroacetate salt rather than the free base. Further work-up using aqueous potassium carbonate yielded the free base in 82 % yield, which was confirmed by the disappearance of the fluorine signal at -75.79 ppm in <sup>19</sup>F NMR.

An initial amination attempt using Gao's method with the ammonium salt yielded poor results, giving only unreacted starting material as the major component in the reaction (Table 1, entry 1). We were not completely surprised by this result, since the  $pK_a$  of the aniline substrate in their system is lower than the  $pK_a$  of our aliphatic amine. In addition, the equivalents of amine we used were found to be lower than reported since the ammonium salt was used at the time.



| entry | <b>22</b> (equiv)      | Pd source (mol %)         | Ligand (mol %)  | Base (equiv)                          | Solvent | Time (h) | Temperature (°C) | <b>23</b> (% yield) | <b>24</b> (% yield) | <b>25</b> (% yield) |
|-------|------------------------|---------------------------|---|---------------------------------------|---------|----------|------------------|---------------------|---------------------|---------------------|
| 1     | <b>22</b> ·[TFA] (1.6) | Pd(OAc) <sub>2</sub> (1)  | P( <sup>t</sup> Bu) <sub>3</sub> ·HBF <sub>4</sub> (2)  | Cs <sub>2</sub> CO <sub>3</sub> (3.1) | Toluene | 24       | 120              | 0                   | 0                   | 0                   |
| 2     | <b>22</b> ·[TFA] (2.5) | Pd(OAc) <sub>2</sub> (5)  | P( <sup>t</sup> Bu) <sub>3</sub> ·HBF <sub>4</sub> (15) | NaO <sup>t</sup> Bu (4.5)             | Xylenes | 16       | 150              | 15                  | 27                  | 30                  |
| 3     | <b>22</b> ·[TFA] (2.5) | Pd(OAc) <sub>2</sub> (5)  | P( <sup>t</sup> Bu) <sub>3</sub> ·HBF <sub>4</sub> (15) | NaO <sup>t</sup> Bu (4.5)             | Xylenes | 48       | 150              | 30                  | 36                  | 0                   |
| 4     | <b>22</b> ·[TFA] (2.5) | Pd(dba) <sub>2</sub> (5)  | P( <sup>t</sup> Bu) <sub>3</sub> ·HBF <sub>4</sub> (15) | NaO <sup>t</sup> Bu (4.5)             | Xylenes | 48       | 150              | 25                  | 37                  | 0                   |
| 5     | <b>22</b> ·[TFA] (2.5) | BrettPhos precatalyst (5) | --  | NaO <sup>t</sup> Bu (4.5)             | Dioxane | 48       | 150              | 0                   | 34                  | 0                   |
| 6     | <b>22</b> (4)          | Pd(OAc) <sub>2</sub> (5)  | P( <sup>t</sup> Bu) <sub>3</sub> ·HBF <sub>4</sub> (15) | NaO <sup>t</sup> Bu (4.5)             | Xylenes | 48       | 150              | 12                  | n.d.                | 0                   |
| 7     | <b>22</b> (4)          | Pd(OAc) <sub>2</sub> (5)  | P( <sup>t</sup> Bu) <sub>3</sub> ·HBF <sub>4</sub> (15) | NaO <sup>t</sup> Bu (4.5)             | Xylenes | 24       | 175 (MW)         | 14                  | 65                  | 0                   |

**Table 1.** Initial optimization efforts of the Buchwald-Hartwig coupling.

Utilizing Kündig's system with the ammonium salt led to the formation of product in 15 % yield (Table 1, entry 2). Two other major products in the reaction were observed: dehalogenated monoaminated product **24** (27 % yield) and monoaminated product **25** (30 % yield). Additional reaction time led to an increase in yield for both **23** and **24** (Table 1, entry 3). We were able to determine the identities of these products by

$^1\text{H}$  NMR (Figure 3). Looking in the aromatic region, the  $^1\text{H}$  of the desired ligand exhibited two signals integrating to two protons each, indicating a symmetric disubstituted aromatic system. With **24**, we were able to see additional signals indicating a monosubstituted aromatic system. Lastly, **25** showed signals indicating an asymmetric disubstituted aromatic system.

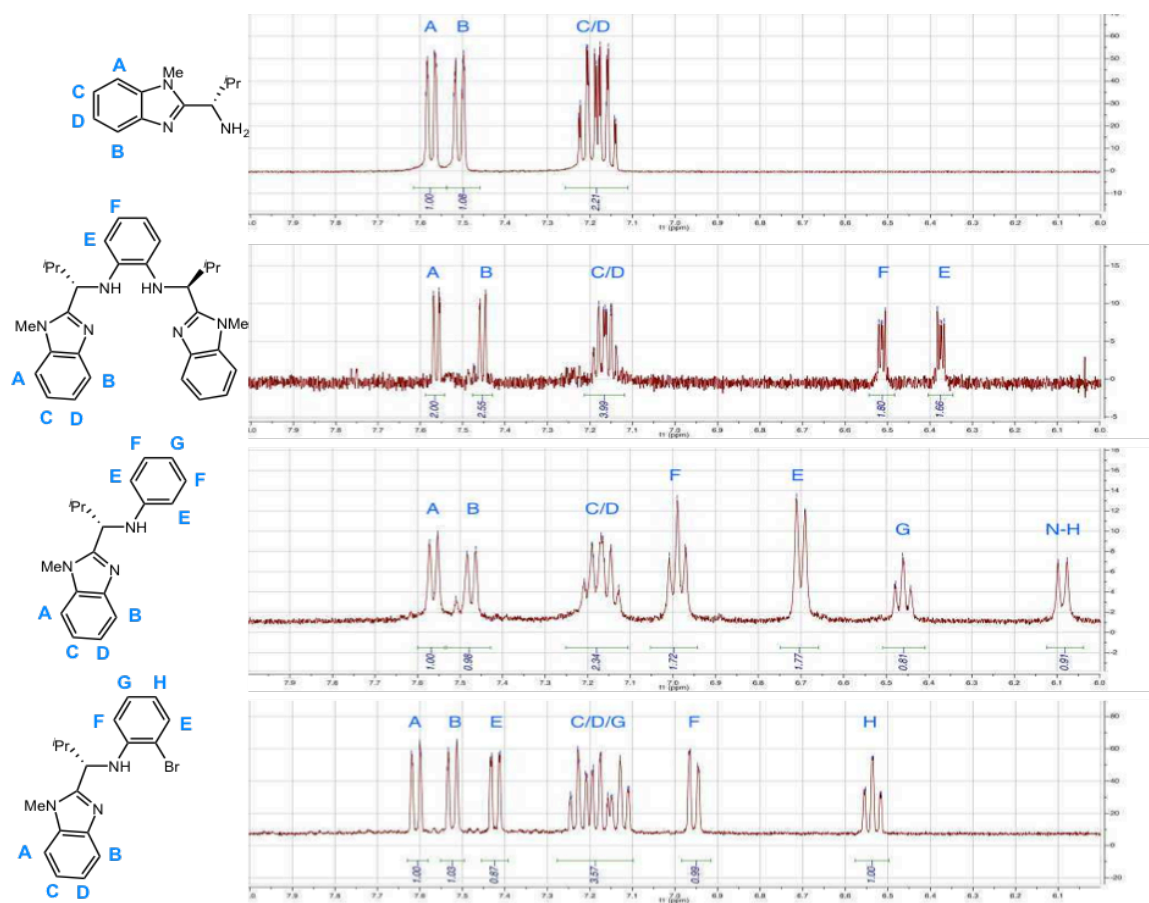


**Figure 3.**  $^1\text{H}$  NMR spectra of Buchwald-Hartwig coupling products compared to starting material.

Alternatively, we also examined the precatalyst palladium source Pd(dba)<sub>2</sub>, which gave a lower yield of **23** and a slight increase for **24** (Table 1, entry 4). We then considered other ligands such as the BrettPhos system, which has been known to efficiently catalyze the Buchwald–Hartwig coupling of primary amines (Table 1, entry 5).<sup>39</sup> However, only **24** was found in low yield, leading us to hypothesize that this system is too bulky to allow the second C–N coupling to occur.

Surprisingly, switching to the free base led to a decrease in yield for **23** when compared to the ammonium salt (Table 1, entry 6). Changing from an oil bath to a microwave system (Table 1, entry 7) led to a slight increase in yield for the product but showed that the yield of dehalogenated monoaminated product increased significantly (65 % yield). Current efforts are focused on continued optimization of the Buchwald-Hartwig reaction, using both the ammonium salt and the free base.

Enough ligand was accumulated in order to explore preliminary metallation reactions to generate Group IX complexes (Figure 4).

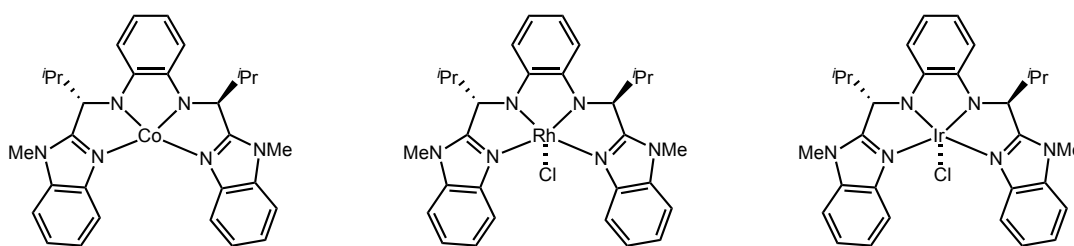
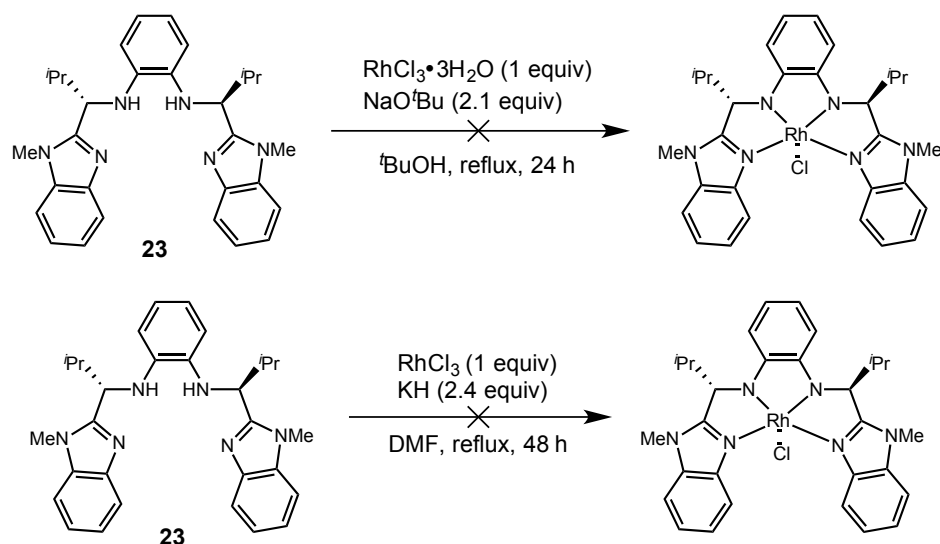


**Figure 4.** Proposed Group IX complexes.

An initial attempt to insert rhodium was made with  $\text{RhCl}_3 \cdot 3\text{H}_2\text{O}$ , but only recovered starting material was isolated (Scheme 24).<sup>40</sup> Switching to the anhydrous version also yielded starting material.



**Scheme 24.** Attempted metallation of **23**.

### III. Future Directions

In conclusion, we are currently developing a novel ligand framework with redox-active capabilities. The modular nature of our ligand allows us to easily modify the backbone using chiral amino acids. We plan to test our new catalyst in a variety of C–H functionalization reactions and expand the scope of these reactions to include difficult-to-control substrates such as acceptor-only diazo compounds and alkyl and aryl azides. Future plans include forming the benzoxazole and the benzothiazole derivatives of our ligand, as well as metallation with other Group IX metals. We are also interested in

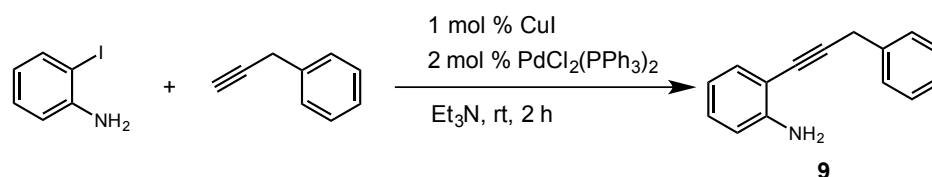
developing an imidazole-based ligand to offset any possible steric issues when forming the Group IX complexes.

## Experimental

**General Information.** All reactions were carried out under an N<sub>2</sub> atmosphere using standard Schlenk techniques unless otherwise stated. All reagents were purchased from Aldrich, Fisher, Strem, or Oakwood Chemicals and used without further purification. Triethylamine was purified by distillation from CaH<sub>2</sub> and stored over 4 Å molecular sieves. Xylenes, dioxane, and *tert*-butanol were purified by distillation from Na/benzophenone ketyl and stored over 4 Å molecular sieves. Anhydrous solvents were purified by passage through activated alumina columns using a *Glass Contours* solvent purification system. Solvents used in workup, extraction, and column chromatography were used as received without further purification. <sup>1</sup>H NMR and <sup>13</sup>C NMR spectra were obtained using Varian Inova 600 spectrometer (600 MHz <sup>1</sup>H, 150 MHz <sup>13</sup>C) and a Varian VNMR 400 spectrometer (400 MHz <sup>1</sup>H, 100 MHz <sup>13</sup>C) in CDCl<sub>3</sub> (neutralized and dried with anhydrous K<sub>2</sub>CO<sub>3</sub>) with internal CHCl<sub>3</sub> as the reference (7.26 ppm for <sup>1</sup>H and 77.23 ppm for <sup>13</sup>C). Chemical shifts ( $\delta$  values) were reported in parts per million (ppm) and coupling constants (*J* values) in Hz. Multiplicity was indicated using the following abbreviations: s = singlet, d = doublet, t = triplet, q = quartet, qn = quintet, m = multiplet, b = broad. Infrared (IR) spectra were recorded using a Thermo Electron Corporation Nicolet 380 FT-IR spectrometer. Melting points were taken using a Fisher Johns melting point apparatus and are uncorrected (dec. = decomposition). High-resolution mass spectra were obtained using a Thermo Electron Corporation Finigan LTQFTMS (at the Mass Spectrometry Facility, Emory University). We acknowledge the use of shared instrumentation provided by grants from the National Institutes of Health and the National Science Foundation. High-pressure liquid chromatography (HPLC) was carried

out on an Agilent 1100 Series equipped with Daicel AD-H, AS-H, OD-H, and OJ-H columns and a variable wavelength detector. Analytical thin layer chromatography (TLC) was performed on precoated glass backed Silicycle 0.25 mm silica gel 60 plates. TLC visualization was accomplished by fluorescence quenching and staining with ethanolic anisaldehyde. Flash column chromatography was carried out using Silicycle SiliaFlash® F60 silica gel (40-63  $\mu\text{m}$ ). Preparatory thin layer chromatography (TLC) was performed on precoated glass backed Silicycle 1000  $\mu\text{m}$  silica gel 60 plates.

### I. Preparation of Azide 7:



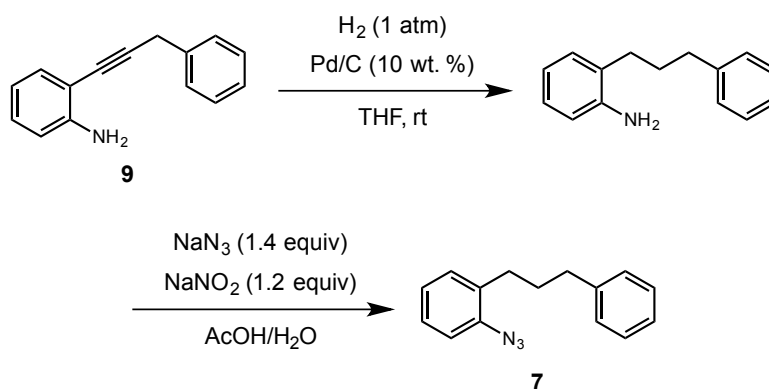
### 2-(3-phenyl-1-propyn-1-yl)aniline (9)

A procedure from literature was adapted as follows.<sup>34</sup> To a flame-dried 100 mL flask was added  $\text{PdCl}_2(\text{PPh}_3)_2$  (126 mg, 0.18 mmol),  $\text{CuI}$  (17 mg, 0.091 mmol), iodoaniline (1.99 g, 9.1 mmol) and 20 mL of triethylamine. 3-phenyl-1-propyne (1.37 mL, 11 mmol) was added dropwise, and the mixture stirred at room temperature for two hours. 50 mL of saturated  $\text{NH}_4\text{Cl}$  and 50 mL of  $\text{CH}_2\text{Cl}_2$  were then added to quench the reaction, and the organic layer was separated. The aqueous layer was extracted two more times with 45 mL of  $\text{CH}_2\text{Cl}_2$ . The combined organic layers were dried with anhydrous  $\text{Na}_2\text{SO}_4$ , filtered, concentrated *in vacuo*. Purification by column chromatography ( $\text{SiO}_2$ , 10 %

EtOAc:hexanes) afforded aniline **9** as an orange oil (1.668 g, 88 %). The spectral data match the literature.

$R_f$  0.5 (20 % EtOAc:hexanes)

$^1\text{H NMR}$  (399 MHz;  $\text{CDCl}_3$ ):  $\delta$  7.42 (d, 2H,  $J = 7.7$  Hz), 7.37-7.24 (m, 4H), 7.11 (t,  $J = 8.1$  Hz, 1H), 6.72-6.66 (m, 2H), 4.18 (bs, 2H), 3.91 (s, 2H).



### 1-azido-2-(3-phenylpropyl)benzene (**7**)

A procedure from literature was adapted as follows.<sup>17</sup> To a flame-dried 50 mL flask was added **2** (0.8 g, 3.86 mmol) and Pd/C (10 wt %, 410 mg, 0.386 mmol) and 27 mL THF. The mixture was vigorously stirred at room temperature under a hydrogen atmosphere for 20 hours. The mixture was filtered through a pad of Celite, washed with  $\text{Et}_2\text{O}$  and concentrated to give 969 mg of crude aniline (4.59 mmol), which was used without further purification.

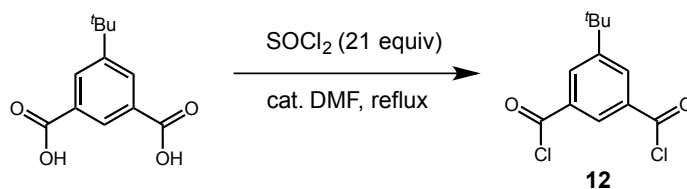
A 50:50 mixture by volume of AcOH and  $\text{H}_2\text{O}$  (48 mL total) was added to the crude aniline and the solution was cooled to  $0^\circ\text{C}$ .  $\text{NaNO}_2$  (380 mg, 5.5 mmol) was added and the resulting mixture was stirred at  $0^\circ\text{C}$  for two hours.  $\text{NaN}_3$  (420 mg, 6.47 mmol) was added and the mixture was warmed to room temperature. After 30 minutes, the mixture

was diluted with 30 mL H<sub>2</sub>O and 30 mL EtOAc. Na<sub>2</sub>CO<sub>3</sub> was slowly added to the biphasic mixture until the pH of the solution was seven. The phases were separated, and the aqueous layer was extracted with EtOAc (2 x 30 mL). The combined organic phases were washed with H<sub>2</sub>O and brine, dried with Na<sub>2</sub>SO<sub>4</sub>, filtered, and concentrated *in vacuo*. Purification by column chromatography (SiO<sub>2</sub>, 10 % EtOAc:hexanes) gave the titled compound as a yellow oil (743 mg, 81 % over two steps). Spectral data match the literature.

**R<sub>f</sub>** 0.84 (20 % EtOAc:hexanes)

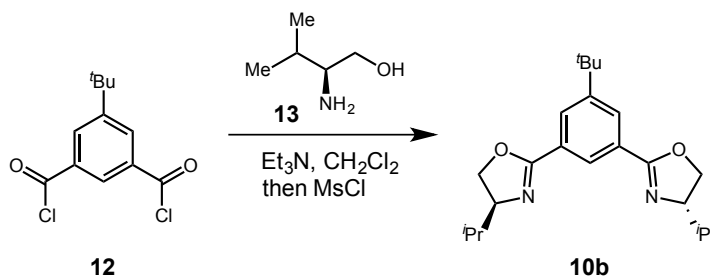
**<sup>1</sup>H NMR** (399 MHz; CDCl<sub>3</sub>): δ 7.30-7.27 (m, 2H), 7.24-7.12 (m, 6H), 7.06 (t, *J* = 8 Hz, 1H), 2.68-2.60 (m, 4H), 1.90 (qn, *J* = 8 Hz, 2H).

## II. Preparation of 5-*tert*-butyl Phebox Ligands



### 5-(*tert*-butyl)isophthaloyl dichloride (12)

A general procedure was adapted as follows.<sup>35</sup> To a flame-dried 100 mL flask was added 5-*tert*-butylisophthalic acid (5.0 g, 22.5 mmol), thionyl chloride (34.3 mL, 472.5 mmol), and DMF (0.1 mL). The mixture was refluxed overnight, then concentrated and dried on high vacuum overnight to give 5-(*tert*-butyl)isophthaloyl dichloride as a pale yellow powder (5.1659 g, 89 %) which was used without further purification.

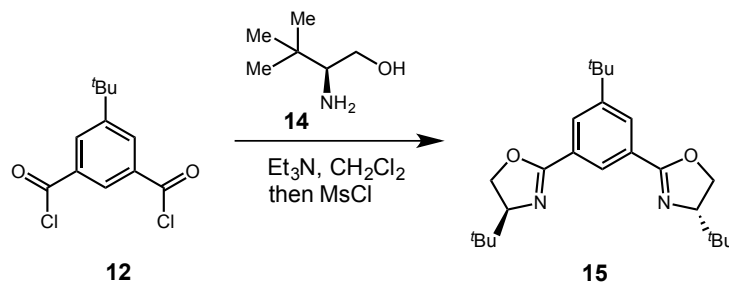


**(*S,S*)-*t*BuPhebox-*i*Pr (**10b**)**

A solution of **12** (619 mg, 2.39 mmol) in CH<sub>2</sub>Cl<sub>2</sub> (9 mL) was slowly added to a cooled (0°C) solution of L-valinol **13** (500 mg, 4.85 mmol), triethylamine (5 mL, 35.85 mmol), and CH<sub>2</sub>Cl<sub>2</sub> (20 mL). The solution was warmed to room temperature and stirred for one hour. It was cooled again to 0°C and methanesulfonyl chloride (0.74 mL, 9.56 mmol) was slowly added to the solution. The solution was warmed to room temperature and stirred overnight. Then 1M K<sub>2</sub>CO<sub>3</sub> (30 mL) was added at 0°C and the mixture was extracted with EtOAc. The organic layer was washed with brine, dried with Na<sub>2</sub>SO<sub>4</sub>, filtered, and concentrated *in vacuo*. Purification by column chromatography (SiO<sub>2</sub>, 30 % EtOAc:hexanes) gave the titled compound as a yellow solid (273 mg, 32 %). Spectral data match the literature.

**R<sub>f</sub>** 0.51 (30 % EtOAc:hexanes)

**<sup>1</sup>H NMR** (399 MHz, CDCl<sub>3</sub>) δ 8.33 (t, *J* = 1.24 Hz, 1H), 8.07 (d, *J* = 1.24 Hz, 2H), 4.47-4.32 (m, 2H), 4.20-4.03 (m, 4H), 1.93-1.78 (m, 2H), 1.36 (s, 9H), 1.02 (d, *J* = 6.7 Hz, 6H), 0.91 (d, *J* = 6.8 Hz, 6H).



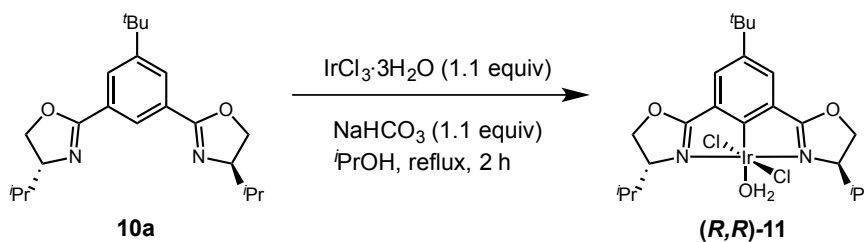
### (*S,S*)-*t*-BuPhebox-*t*-Bu (15)

A solution of **12** (553 mg, 2.13 mmol) in CH<sub>2</sub>Cl<sub>2</sub> (8.5 mL) was slowly added to a cooled (0°C) solution of *S*-*tert*-leucinol (500 mg, 4.27 mmol), triethylamine (4.5 mL, 32 mmol) in CH<sub>2</sub>Cl<sub>2</sub> (17 mL). The solution was warmed to room temperature and stirred for one hour. It was cooled again to 0°C and methanesulfonyl chloride (0.66 mL, 8.53 mmol) was slowly added to the solution. The solution was warmed to room temperature and stirred overnight. Then 1M K<sub>2</sub>CO<sub>3</sub> (28 mL) was added at 0°C and the mixture was extracted with EtOAc (30 mL). The organic layer was washed with brine, dried with Na<sub>2</sub>SO<sub>4</sub>, filtered, and concentrated *in vacuo*. Purification by column chromatography (SiO<sub>2</sub>, 30 % EtOAc:hexanes) gave the titled compound as a white solid (443 mg, 54 %). Spectral data match the literature.

**R<sub>f</sub>** 0.71 (30 % EtOAc:hexanes)

**<sup>1</sup>H NMR** (399 MHz, CDCl<sub>3</sub>) δ 8.37 (t, *J* = 1.6 Hz, 1H), 8.06 (d, *J* = 1.6 Hz, 2H), 4.35 (dd, *J* = 10.1, 8.6 Hz, 2H), 4.24 (dd, *J* = 8.6, 7.6 Hz, 2H), 4.06 (dd, *J* = 10.1, 7.6 Hz, 2H), 1.37 (s, 9H), 0.96 (s, 18H).

### III. Preparation of 4-*tert*-butyl Iridium(III) Phebox Complexes

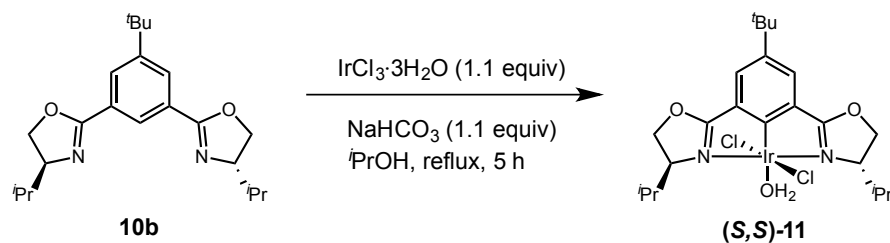


#### **[(*R,R*)-*t*BuPhebox-*i*Pr]IrCl<sub>2</sub>(H<sub>2</sub>O) (*R,R*)-11**

A general procedure was adapted as follows.<sup>11</sup> To a flame-dried 50 mL flask was added **10a** (200 mg, 0.56 mmol), IrCl<sub>3</sub>·3H<sub>2</sub>O (218 mg, 0.62 mmol), NaHCO<sub>3</sub> (52 mg, 0.62 mmol), and *i*PrOH (19 mL). The mixture was refluxed for two hours, then concentrated and adsorbed onto silica gel, and purified using column chromatography (gradient: 20 % EtOAc:hexanes → 70 %). The fractions at R<sub>f</sub> 0.31 (SiO<sub>2</sub>, 50 % EtOAc:hexanes) were collected and concentrated and crystallized by slow diffusion of pentane into a saturated CH<sub>2</sub>Cl<sub>2</sub> mixture to give the titled compound as an orange solid (46.8 mg, 13 %).

**R<sub>f</sub>** 0.31 (50 % EtOAc:hexanes)

**<sup>1</sup>H NMR** (400 MHz, CDCl<sub>3</sub>) δ 7.51 (s, 2H), 4.93-4.74 (m, 4H), 4.36-4.13, (m, 2H), 2.43 (s, 2H), 1.37 (s, 9H), 0.97 (dd, *J* = 19.1, 7.0 Hz, 12H).



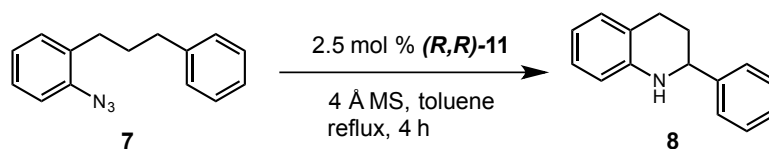
**[(S,S)-<sup>t</sup>BuPhebox-<sup>i</sup>Pr]IrCl<sub>2</sub>(H<sub>2</sub>O) (S,S)-11**

To a flame-dried 50 mL flask was added **10b** (273 mg, 0.765 mmol), IrCl<sub>3</sub>·3H<sub>2</sub>O (0.2965 g, 0.842 mmol), NaHCO<sub>3</sub> (0.071 g, 0.842 mmol), and *i*PrOH (26 mL). The mixture was refluxed for five hours, then concentrated and adsorbed onto silica gel, and purified using column chromatography (SiO<sub>2</sub>, gradient: 30 % EtOAc:hexanes → 70 %). The fractions at R<sub>f</sub> 0.31 (50 % EtOAc:hexanes) were collected and concentrated and crystallized by slow diffusion of pentane into a saturated CH<sub>2</sub>Cl<sub>2</sub> mixture to give the titled compound as an orange solid (139 mg, 29 %).

R<sub>f</sub> 0.31 (50 % EtOAc:hexanes)

<sup>1</sup>H NMR (400 MHz, CDCl<sub>3</sub>) δ 7.51 (s, 2H), 4.84 (p, *J* = 9.1 Hz, 4H), 4.25 (s, 2H), 2.43 (s, 2H), 1.36 (s, 9H), 0.97 (dd, *J* = 18.0, 7.0 Hz, 12H).

#### IV. Amination Reaction for Tetrahydroquinoline Formation<sup>17</sup>

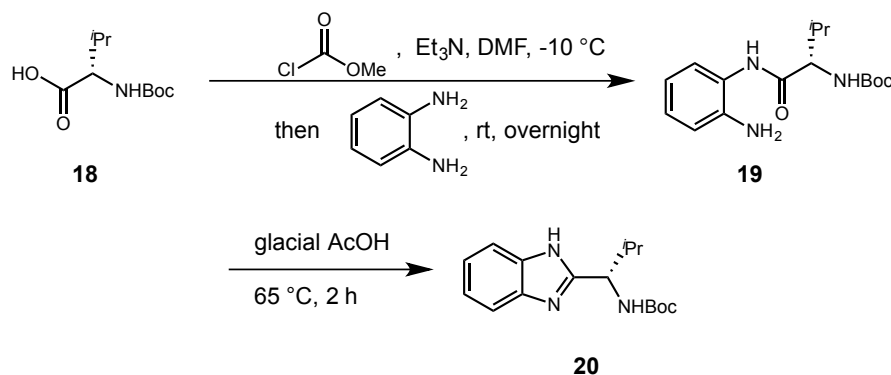


To a flame-dried 10 mL flask with activated powdered 4 Å molecular sieves was added **7** (37.5 mg, 0.16 mmol), **(R,R)-11** (2.5 mg, 2.5 mol %) and toluene (3.2 mL). The mixture was refluxed for four hours. After cooling to room temperature, the mixture was then filtered through celite, concentrated, and purified by preparatory thin layer chromatography (10 % EtOAc:hexanes). The band at  $R_f$  0.65 was collected and concentrated to give tetrahydroquinoline **4** (3 mg, 9 %, 58:42 er). Spectral data match the literature. The enantiomeric ratio was determined by chiral HPLC.

**<sup>1</sup>H NMR** (400 MHz, CDCl<sub>3</sub>)  $\delta$  7.46-7.25 (m, 5H), 7.02 (m, 2H), 6.66 (td,  $J = 7.4, 1.2$  Hz, 1H), 6.61-6.49 (m, 1H), 4.45 (dd,  $J = 9.4, 3.3$  Hz, 1H), 4.05 (s, 1H), 3.01-2.86 (m, 1H), 2.74 (dt,  $J = 16.3, 4.7$  Hz, 1H), 2.13 (m, 1H), 2.00 (m, 1H).

**HPLC** (Daicel AS-H, 254 nm detection, 5 % 2-propanol:hexanes, 1 mL/min);  $t_R = 5.50$  min (major) and 13.75 min (minor).

## V. Preparation of Ligand 23



### *tert*-butyl (*S*)-(1-(1*H*-benzo[*d*]imidazol-2-yl)-2-methylpropyl)carbamate (**20**)

Procedure from literature was modified as follows.<sup>28</sup> To a flame-dried 100 mL flask was added Boc-*L*-valine **18** (3.23 g, 14.9 mmol), triethylamine (2.1 mL, 14.9 mmol), and anhydrous DMF (13 mL). The mixture was cooled to -10 °C, and methyl chloroformate (1.15 mL, 14.9 mmol) was added dropwise. After stirring at -10 °C for 20 minutes, *o*-phenylenediamine (1.61 g, 14.9 mmol) was added in parts. The resulting mixture was warmed to room temperature and stirred overnight. Then the mixture was diluted with Et<sub>2</sub>O (40 mL) and extracted with H<sub>2</sub>O. The aqueous layer was back-extracted with Et<sub>2</sub>O (2 x 100 mL), and the combined organic layers were washed with H<sub>2</sub>O (2x), 5 % LiCl, saturated NaHCO<sub>3</sub>, H<sub>2</sub>O, and brine. The organic layer was dried with Na<sub>2</sub>SO<sub>4</sub>, filtered, and concentrated to give **17** as a crude yellow solid (4.15 g) which was used without further purification.

To a 50 mL flask was added **19** (3.83 g, 12.5 mmol) and glacial AcOH (6.25 mL). The solution was stirred at 65 °C for two hours, and was then cooled to room temperature. The AcOH was removed by high vacuum over several hours and the resulting crude

mixture was dissolved in EtOAc (100 mL) and washed with H<sub>2</sub>O and saturated NaHCO<sub>3</sub>. The organic layer was dried with Na<sub>2</sub>SO<sub>4</sub>, filtered, concentrated, and crystallized in a mixture of CHCl<sub>3</sub>/hexanes to give **20** as a white solid (2.3 g, 53 % over two steps).

**<sup>1</sup>H NMR** (400 MHz, CDCl<sub>3</sub>) δ 10.59 (s, 1H), 7.80-7.64 (m, 1H), 7.43-7.29 (m, 1H), 7.25-7.13 (m, 2H), 5.60 (d, *J* = 8.7 Hz, 1H), 4.60 (t, *J* = 8.4 Hz, 1H), 2.58-2.36 (m, 1H), 1.43 (s, 9H), 1.06 (d, *J* = 6.7 Hz, 3H), 0.93 (d, *J* = 6.7 Hz, 4H).

**<sup>13</sup>C NMR** (101 MHz, CDCl<sub>3</sub>) δ 156.63, 154.82, 133.40, 122.97, 122.24, 119.46, 111.15, 80.41, 77.55, 77.43, 77.23, 76.91, 56.03, 32.07, 28.56, 19.79, 19.11.

**HRMS** [+NSI] calculated for C<sub>16</sub>H<sub>24</sub>O<sub>2</sub>N<sub>3</sub> 290.1863, found 290.1859 [M+H]<sup>+</sup>

**IR** (thin film, cm<sup>-1</sup>) 3142, 2973, 1672, 1288

**[α]<sub>D</sub><sup>20</sup>** -207.9 (*c* = 1.00, THF)

**m.p.** 250 °C (dec.)



***tert*-butyl (*S*)-(2-methyl-1-(1-methyl-1*H*-benzo[*d*]imidazol-2-yl)propyl)carbamate (21)**

To a flame-dried 250 mL flask was added **20** (2.3 g, 8.06 mmol) and THF (42 mL). The solution was cooled to -78 °C and LiHMDS (1 M in hexanes, 8.06 mL, 8.06 mmol) was added over the course of 30 minutes using a syringe pump. After stirring an additional 30 minutes at -78 °C, methyl iodide (0.53 mL, 8.45 mmol) was added dropwise. The mixture was warmed to room temperature and stirred overnight. The next day, the solution was

quenched with H<sub>2</sub>O and extracted with EtOAc (3 x 40 mL). The combined organic layers were dried, concentrated, and purified by column chromatography (SiO<sub>2</sub>, 20 % EtOAc:hexanes → 25 %) to give **21** as a white crystalline solid (2.14 g, 87 %, 96 % brsm).

<sup>1</sup>H NMR (400 MHz, CDCl<sub>3</sub>) δ 7.78-7.67 (m, 1H), 7.43-7.32 (m, 1H), 7.32-7.25 (m, 2H), 5.41 (d, *J* = 9.5 Hz, 1H), 4.80 (t, *J* = 9.6 Hz, 1H), 3.83 (s, 3H), 2.28 (m, 1H), 1.41 (s, 9H), 1.05 (d, *J* = 6.7 Hz, 3H), 0.93 (d, *J* = 6.7 Hz, 3H).

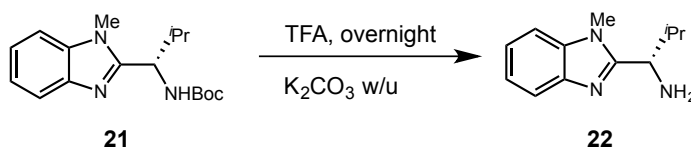
<sup>13</sup>C NMR (101 MHz, CDCl<sub>3</sub>) δ 155.33, 142.64, 122.81, 122.49, 119.72, 109.81, 80.00, 52.60, 33.81, 30.33, 28.65, 19.92, 18.71.

HRMS [+NSI] calculated for C<sub>17</sub>H<sub>26</sub>O<sub>2</sub>N<sub>3</sub> 304.2020, found 304.2016 [M+H]<sup>+</sup>

IR (thin film, cm<sup>-1</sup>) 3195, 2965, 1693, 1267

[α]<sub>D</sub><sup>20</sup> -120.4 (*c* = 1.00, CHCl<sub>3</sub>)

m.p. 110-112 °C



**(S)-2-methyl-1-(1-methyl-1H-benzo[d]imidazol-2-yl)propan-1-amine (22)**

To a dried 7 mL vial was added **21** (1.3062 g, 4.3 mmol) and TFA (4.89 mL). The mixture was stirred at room temperature for 20 hours, and then dissolved in EtOAc (30 mL) and quenched with 1 M K<sub>2</sub>CO<sub>3</sub>. The phases were separated, and the aqueous layer

was extracted with EtOAc (3 x 40 mL). The combined organic layers were dried with Na<sub>2</sub>SO<sub>4</sub>, filtered, and concentrated to give **22** as a pale yellow solid (542 mg, 62 %).

**<sup>1</sup>H NMR** (400 MHz, CDCl<sub>3</sub>) δ 7.77-7.71 (m, 1H), 7.36-7.31 (m, 1H), 7.30-7.26 (m, 2H), 3.92 (d, *J* = 6.9 Hz, 1H), 3.80 (s, 3H), 2.17 (h, *J* = 6.8 Hz, 1H), 1.75 (s, 2H), 1.06 (d, *J* = 6.7 Hz, 3H), 0.95 (d, *J* = 6.8 Hz, 3H).

**<sup>13</sup>C NMR** (101 MHz, DMSO-*d*<sub>6</sub>) δ 158.78, 142.84 , 136.65, 122.49 , 122.21 , 119.44 , 110.89 , 54.33 , 34.17 , 30.67 , 20.69 , 19.12.

**HRMS** [+NSI] calculated for C<sub>12</sub>H<sub>18</sub>N<sub>3</sub> 204.1495, found 204.1491 [M+H]<sup>+</sup>

**IR** (thin film, cm<sup>-1</sup>) 3363, 3289, 2949, 1676, 1467, 1441

**[α]<sub>D</sub><sup>20</sup>** +47.9 (*c* = 1.00, CHCl<sub>3</sub>)

**m.p.** 84-86 °C

### Determination of the absolute configuration for amine **22**.

Absolute configuration of the free base was determined by Mosher's amide analysis, where the  $^1\text{H}$  signal for the methine proton of the isopropyl group shifted with regards to the enantiomer of the acid chloride used (Figure 5). Based off the example shown by Priest *et al.* (Figure 5a),<sup>41</sup> the downfield shift of the methine peak for the (*R*)-amide and the upfield shift for the (*S*) amide led to the conclusion that the (*S*) enantiomer was the one synthesized (Figure 5b).

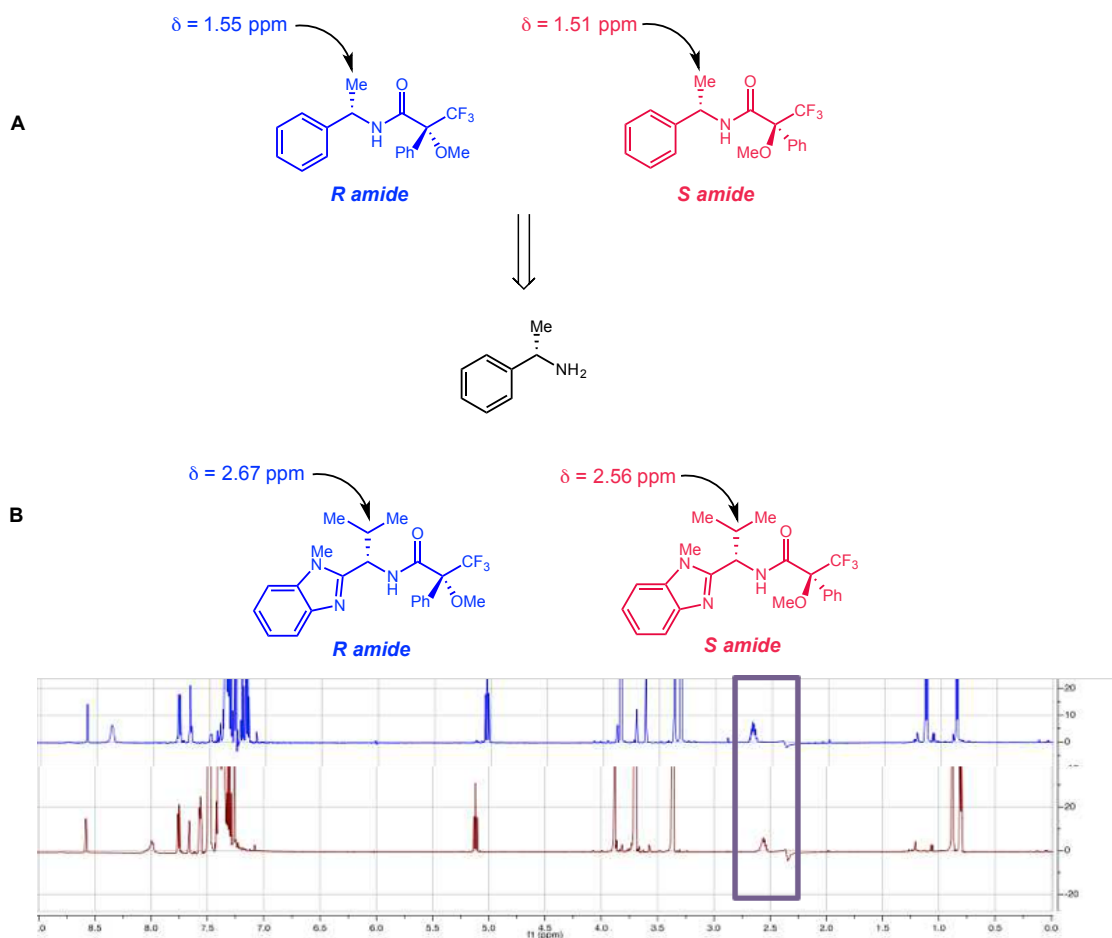
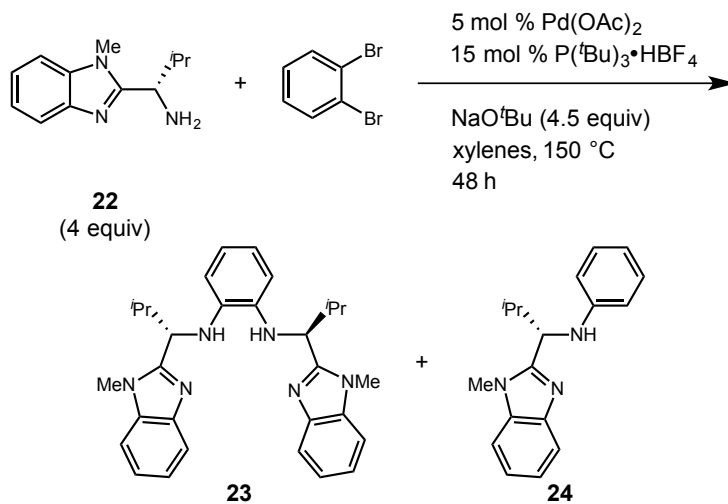


**Figure 5.** Mosher amide analysis for absolute configuration of amine **22**.

***N*<sup>1</sup>,*N*<sup>2</sup>-bis((*S*)-2-methyl-1-(1-methyl-1*H*-benzo[*d*]imidazol-2-yl)propyl)benzene-1,2-diamine (**23**)**



General Buchwald-Hartwig procedure was adapted from literature as follows.<sup>38</sup> To a flame-dried sealed tube was added **22** (81 mg, 0.4 mmol), Pd(OAc)<sub>2</sub> (1.1 mg, 0.005 mmol), P(<sup>t</sup>Bu)<sub>3</sub>·HBF<sub>4</sub> (4.3 mg, 0.015 mmol), and NaO<sup>t</sup>Bu (43 mg, 0.45 mmol). Degassed xylenes (freeze-pump-thaw, 3x, 0.8 mL) and 1,2-dibromobenzene (0.012 mL, 0.1 mmol) were added. The mixture was stirred at room temperature for 30 minutes, placed in a preheated oil bath at 155 °C, and stirred for 48 hours. The mixture was then cooled to room temperature, filtered through celite, and the xylenes was removed using high vacuum overnight. The remaining mixture was dissolved in EtOAc, adsorbed onto silica, and purified using column chromatography (SiO<sub>2</sub>, gradient: 20 % EtOAc:hexanes → 40 %). The fractions at R<sub>f</sub> 0.03 (40 % EtOAc:hexanes) were collected and concentrated to give **23** as a yellow solid(14.5 mg, 30 %).

**R<sub>f</sub>** 0.03, (40 % EtOAc:hexanes)

**<sup>1</sup>H NMR** (600 MHz, DMSO-*d*<sub>6</sub>) δ 7.63-7.54 (m, 2H), 7.52-7.43 (m, 2H), 7.26-7.10 (m, 4H), 6.53 (dd, *J* = 5.9, 3.5 Hz, 2H), 6.39 (dd, *J* = 5.9, 3.5 Hz, 2H), 5.12 (d, *J* = 9.0 Hz, 2H), 4.57 (t, *J* = 8.6 Hz, 2H), 3.73 (s, 6H), 2.45-2.41 (m, 2H), 1.22 (d, *J* = 6.6 Hz, 6H), 0.91 (d, *J* = 6.7 Hz, 6H).

**<sup>13</sup>C NMR** (101 MHz, DMSO-*d*<sub>6</sub>) δ 157.22, 142.80, 137.56, 136.69, 122.59, 122.37, 119.66, 119.46, 114.66, 110.97, 58.36, 33.55, 30.69, 20.55.

**IR** (thin film, cm<sup>-1</sup>) 2960, 2927, 1465, 740

**HRMS** [+NSI] calculated for C<sub>30</sub>H<sub>37</sub>N<sub>6</sub> 481.3074, found 481.3079 [M+H]<sup>+</sup>

**[α]<sub>D</sub><sup>20</sup>** -2.1 (*c* = 1.00, CHCl<sub>3</sub>)

**m.p.** 61-63 °C

Fractions at R<sub>f</sub> 0.57 (40 % EtOAc:hexanes) were also collected and concentrated to give **24** as a yellow solid (10 mg, 36 %).

**R<sub>f</sub>** 0.57 (40 % EtOAc:hexanes)

**<sup>1</sup>H NMR** (600 MHz, DMSO-*d*<sub>6</sub>) δ 7.56 (d, *J* = 7.8 Hz, 1H), 7.47 (d, *J* = 7.8 Hz, 1H), 7.22-7.12 (m, 2H), 6.99 (t, *J* = 8.6 Hz, 2H), 6.70 (d, *J* = 7.6 Hz, 2H), 6.46 (t, *J* = 7.2 Hz, 1H), 6.07 (d, *J* = 8.5 Hz, 1H), 4.53 (t, *J* = 8.4 Hz, 1H), 2.37-2.28 (m, 1H), 1.11 (d, *J* = 6.7 Hz, 3H), 0.83 (d, *J* = 6.7 Hz, 3H).

**<sup>13</sup>C NMR** (101 MHz, CDCl<sub>3</sub>) δ 155.72, 147.79, 142.48, 135.87, 129.50, 122.51, 122.26, 119.67, 118.28, 113.82, 109.40, 57.72, 34.15, 30.41, 19.78, 19.58

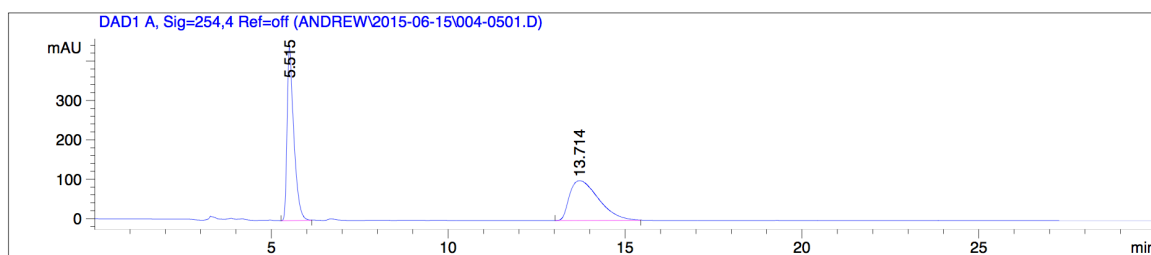
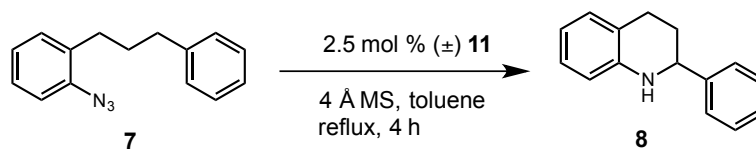
**HRMS** [+NSI] calculated for C<sub>18</sub>H<sub>22</sub>N<sub>3</sub> 280.1808, found 280.1808 [M+H]<sup>+</sup>

**IR** (thin film, cm<sup>-1</sup>) 3253, 3013, 2960, 2925, 1601, 1464

**[α]<sub>D</sub><sup>20</sup>** -0.8 (*c* = 1.00, CHCl<sub>3</sub>)

**m.p.** 154-160 °C

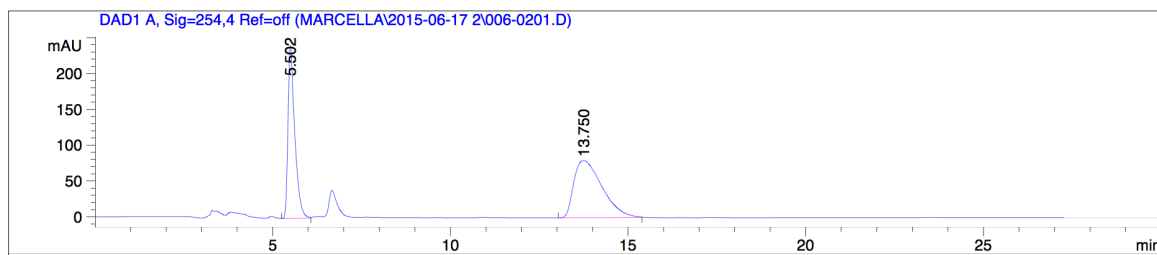
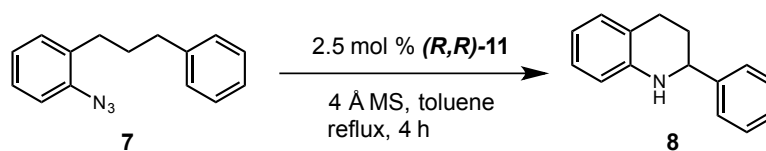
## VI. HPLC data



Signal 1: DAD1 A, Sig=254,4 Ref=off

| Peak # | RetTime [min] | Type | Width [min] | Area [mAU*s] | Height [mAU] | Area %  |
|--------|---------------|------|-------------|--------------|--------------|---------|
| 1      | 5.515         | VB   | 0.1900      | 5729.61865   | 439.77795    | 49.8743 |
| 2      | 13.714        | BB   | 0.8870      | 5758.50928   | 101.02355    | 50.1257 |

Totals : 1.14881e4 540.80151



Signal 1: DAD1 A, Sig=254,4 Ref=off

| Peak # | RetTime [min] | Type | Width [min] | Area [mAU*s] | Height [mAU] | Area %  |
|--------|---------------|------|-------------|--------------|--------------|---------|
| 1      | 5.502         | VB   | 0.1903      | 3149.39502   | 241.29436    | 41.7473 |
| 2      | 13.750        | BB   | 0.8485      | 4394.54932   | 79.79990     | 58.2527 |

Totals : 7543.94434 321.09426

## References

1. Liang, X.; Jiang, S.-Z.; Wei, K.; Yang, Y.-R. *J. Am. Chem. Soc.* **2016**, *138*, 2560.
2. Li, F.; Tartakoff, S. S.; Castle, S. L. *J. Am. Chem. Soc.*, **2009**, *131*, 6674.
3. Horning, B. D.; MacMillan, D. W. C. *J. Am. Chem. Soc.*, **2013**, *135*, 6442.
4. Baumann, M.; Baxendale, I. R. *Beilstein J. Org. Chem.*, **2013**, *9*, 2265.
5. Davies, H. M. L.; Beckwith, R. E. *J. Chem. Rev.* **2003**, *103*, 2861.
6. Davies, H. M. L.; Grazini, M. V. A.; Aouad, E. *Org. Lett.* **2001**, *3*, 1475.
7. Wang, H.; Li, G.; Engle, K. M.; Yu, J. Q.; Davies, H. M. L. *J. Am. Chem. Soc.* **2013**, *135*, 6774.
8. Doyle, M. P.; Phillips, I. M. *Tetrahedron Lett.* **2001**, *42*, 3155.
9. Bode, J. W.; Doyle, M. P.; Protopopova, M. N.; Zhou, Q.-L. *J. Org. Chem.* **1996**, *61*, 9146.
10. Takahashi, T.; Tsutsui, H.; Tamura, M.; Kitagaki, S.; Nakajima, M.; Hashimoto, S. *Chem. Commun.* **2001**, *17*, 1604.
11. Müller, P.; Tohill, S. *Tetrahedron* **2000**, *56*, 1725.
12. Espino, C. G.; Wehn, P. M.; Chow, J.; Du Bois, J. *J. Am. Chem. Soc.* **2001**, *123*, 6935.
13. Kurokawa, T.; Kim, M.; Du Bois, J. *Angew. Chem. Int. Ed.* **2009**, *48*, 2777.
14. Hinman, A.; Du Bois, J. *J. Am. Chem. Soc.* **2003**, *125*, 11510.
15. Kim, J. Y.; Park, S. H.; Ryu, J.; Cho, S. H.; Kim, S. H.; Chang, S. *J. Am. Chem. Soc.* **2012**, *134*, 9110.
16. Kang, T.; Kim, Y.; Lee, D.; Wang, Z.; Chang, S. *J. Am. Chem. Soc.* **2014**, *136*, 4141.

17. Sun, K.; Sachwani, R.; Richert, K. J.; Driver, T. G. *Org. Lett.* **2009**, *11*, 3598.
18. Unpublished work by Nina Weldy and Clay Owens.
19. Villanueva, O.; Weldy, N. M.; Blakey, S. B.; MacBeth, C. E. *Chem. Sci.* **2015**, *6*, 6672.
20. Chen, Y.; Ruppel, J. V.; Zhang, X. P. *J. Am. Chem. Soc.* **2007**, *129*, 12074.
21. Zhu, S.; Ruppel, J. V.; Lu, H.; Wojtas, L.; Zhang, X. P. *J. Am. Chem. Soc.* **2008**, *130*, 5042.
22. Zhu, S.; Perman, J. A.; Zhang, X. P. *Angew. Chem. Int. Ed.* **2008**, *47*, 8460.
23. Ruppel, J. V.; Gauthier, T. J.; Snyder, N. L.; Perman, J. A.; Zhang, X. P. *Org. Lett.* **2009**, *11*, 2273.
24. Zhu, S.; Xu, X.; Perman, J. A.; Zhang, X. P. *J. Am. Chem. Soc.* **2010**, *132*, 12796.
25. Cui, X.; Xu, X.; Lu, H.; Zhu, S.; Wojtas, L.; Zhang, X. P. *J. Am. Chem. Soc.* **2011**, *133*, 3304.
26. Lu, H.; Dzik, W. I.; Xu, X.; Wojtas, L.; de Bruin, B.; Zhang, X. P. *J. Am. Chem. Soc.* **2011**, *133*, 8518.
27. Cui, X.; Xu, X.; Wojtas, L.; Kim, M. M.; Zhang, X. P. *J. Am. Chem. Soc.* **2012**, *12*, 19981.
28. Pellissier, H.; Clavier, H. *Chem. Rev.* **2014**, *114*, 2775.
29. Cui, X.; Xu, X.; Jin, L.-M.; Wojtas, L.; Zhang, X. P. *Chem. Rev.* **2015**, *6*, 1219.
30. Zheng, C.; You, S.L. *RSC Adv.*, **2014**, *4*, 6173.
31. Hennessy, E. T.; Betley, T. A. *Science*, **2013**, *340*, 591.
32. Suematsu, H.; Kanchiku, S.; Uchida, T.; Katsuki, T. *J. Am. Chem. Soc.* **2008**, *130*, 10327.

33. Suematsu, H.; Katsuki, T. *J. Am. Chem. Soc.* **2009**, *131*, 14218.
34. Saito, T.; Nihei, H.; Otani, T.; Suyama, T.; Furukawa, N.; Saito, M. *Chem. Commun.* **2008**, *2*, 172.
35. Owens, C. P.; Varela-Álvarez, A.; Boyarskikh, V.; Musaev, D. G.; Davies, H. M. L.; Blakey, S. B. *Chem. Sci.* **2013**, *4*, 2590.
36. Mohite, P. H.; Drabina, P.; Bureš, F. *Synlett.* **2014**, *25*, 491.
37. Dai, W.; Li, J.; Li, G.; Yang, H.; Wang, L.; Gao, S. *Org. Lett.* **2013**, *15*, 4138.
38. Jia, Y.-X.; Katayev, D.; Bernardinelli, G.; Seideil, T. M.; Kündig, E. P. *Chem. Eur. J.* **2010**, *16*, 6300.
39. Maiti, D.; Fors, B. P.; Henderson, J. L.; Nakamura, Y.; Buchwald, S. L. *Chem. Sci.* **2010**, *2*, 57.
40. Stinziano-Eveland, R. A.; Liable-Sands, L. M.; Rheingold, A. L.; Nguyen, S. T. *Inorg. Chem.* **2000**, *39*, 2452.
41. Allen, D. A.; Tomaso Jr., A. E.; Priest, O. P.; Hindson, D. F.; Hurlburt, J. L. *J. Chem. Educ.* **2008**, *85*, 698.